Smart Structures and Systems, *Vol. 27, No. 5 (2021) 871-890*
DOI: https://doi.org/10.12989/sss.2021.27.5.871

Influence of crack on the permeability of plastic concrete

Yongqiang He [1], Rayed Alyousef [2], Abdulaziz Alaskar [3], Hisham Alabduljabbar [2], Abdeliazim Mustafa Mohamed [2], Nelson Maureira-Carsalade [4], Angel Roco-Videla [5], Alibek Issakhov [6,7] and Hamid Assilzadeh*[8]

[1] *Yiwu Industrial & Commercial College, Yiwu, Zhejiang 322000, P.R. China*
[2] *Department of Civil Engineering, College of Engineering, Prince Sattam bin Abdulaziz University, Al-kharj 11942, Saudi Arabia*
[3] *Department of Civil Engineering, College of Engineering, King Saud University, Riyadh 11362, Saudi Arabia*
[4] *Facultad de Ingeniería, Universidad Católica de la Santísima Concepción, Chile*
[5] *Programa Magister en ciencias químico-biológicas, Facultad de Ciencias de la Salud, Universidad Bernardo O´Higgins, Santiago, Chile*
[6] *Al-Farabi Kazakh National University, Almaty, Kazakhstan*
[7] *Kazakh-British Technical University, Almaty, Kazakhstan*
[8] *Institute of Research and Development, Duy Tan University, Da Nang 550000, Vietnam*

(*Received December 5, 2019, Revised February 15, 2020, Accepted March 12, 2021*)

Abstract. This study examined the relations between permeability of the concrete due to addition of new cracks. The different concrete types analyzed were standard concrete, reinforced steel fiber concrete, and reinforced concrete polypropylene fiber. In consideration of the improved polypropylene content of polypropylene fiber reinforced concrete, the crack diameter was decreased by 72-93% for up to 0.25% fiber and cracks were eliminated with 0.3% fiber inclusion. In terms of steel fiber-reinforced concrete, the results showed that steel reinforcing macro fibers decrease the permeability of cracked concrete at wider crack widths. While the permeability of unreinforced concrete was the highest, 0.5% steel content resulted in lower permeability while a higher steel content concrete with 1% steel had the lowest permeability. Crack stitching phenomenon and the effect of multiple cracks may be attributed to the decrease in the permeability. With respect to normal concrete, the findings showed the crack opening displacement at the highest tension is less than 20 microns. At this loading stage, after unloading, around 80% of the displacement is restored and the residual crack opening is notably small, indicating the low impact of cracking on concrete permeability (CP) and showing that CP was increased with crack width. As a result, adding polypropylene aggregate to concrete could significantly reduce the width of crack, while adding steel fiber to concrete reduces the permeability of cracked concrete compared to normal concrete which may result in a minor crack on CP.

Keywords: plastic concrete; permeability; crack; water to cement ratio (W/C); bentonite to cement ratio (B/C)

1. Introduction

Since the ground is always subjected to seepage of water or contaminant flows, cutoff walls are one of the most efficient tools which have been introduced for tightening the ground against these factors. They are employed in different geotechnical structures such as the landfill underground barrier and dam foundation (DF) (Soroush and Soroush 2005). The material for producing cutoff walls is the same as that of normal concrete, however, due to the embedding in a relatively soft medium of soil, the cutoff wall should be adopted with adjacent media and therefore, the stiffness ratio of the two different media should be limited to a certain amount (ICOLD 1985). For this purpose, the betonies are added to the concrete mixture to produce concrete with specified specifications such as; lower stiffness and higher failure strain, which is represented as plastic concrete. Besides, the other characteristics determined for plastic concrete are sufficient strength and the lower permeability (Chen *et al*. 2017, Afsar Dizaj *et al*. 2018, He *et al*. 2018a, b, Han *et al*. 2019, 2020, Chen *et al*. 2021b). Due to the interaction with the dam's body and the surrounded ground, the plastic cutoff wall is subjected to different external loads (Pisheh and Hosseini 2012, Cheng *et al*. 2016, Chen *et al*. 2018, Gao and Zhang 2019, Liu *et al*. 2019, He *et al*. 2020a, Jiao *et al*. 2020a, Li *et al*. 2020c, Liu *et al*. 2020f). In addition, hydrostatic loads of reservoir lead to some stress and deformation in the cutoff wall. These loads happen during the first impounding and sequent fluctuation in the reservoir (Hinchberger *et al*. 2010, Yang and Sowmya 2015, Xu *et al*. 2018b, Wu *et al*. 2019a, Gao and Lu 2020, Jiao *et al*. 2020b, Zuo *et al*. 2020a, b). The stress and strain in the cutoff wall are induced by these interactions and eventually may exceed the limit value and result in forming a crack in plastic concrete. The performance of the cutoff wall is weakened by this crack, which leads to creation of a passage for water seepage (Yang *et al*. 2018, Zhu *et al*. 2019a, b, Abedini *et al*. 2020a, Huang *et al*. 2020b, c, Ju *et al*. 2020, Ni *et al*. 2020, Sun *et al*. 2020, Wang *et al*. 2020b). The erosion in cutoff wall material results from the continuous seepage through the cracks and consequently

*Corresponding author, Ph.D.,
E-mail: hamidassilzadeh@duytan.edu.vn

ISSN: 1738-1584 (Print), 1738-1991 (Online)

leads to increasing the dimension of crack. The other factors that can create and extend cracks in cutoff wall are; higher hydraulic gradient at the connection areas between dam's core and the cutoff wall (Rice and Duncan 2009, Zuo *et al*. 2015, 2017, Jiang *et al*. 2018, Xu *et al*. 2018a, Guan *et al*. 2019, Lv and Song 2019, Lv and Xiu 2019, Tsai *et al*. 2019, Lv and Qiao 2020), stress concentration because of major change in stiffness of the cutoff wall and foundation (Mahboubi and Ajorloo 2005), low quality of concrete during construction and slippage of the trench wall during filling. Although the possibility of cracks in plastic concrete is high and leads to increasing the water seepage, determining the cutoff wall permeability is according to the obtained results performed on the intact specimen, which may result in underestimating the seepage through DF (Wang *et al*. 2015, Li *et al*. 2019b, Zhao *et al*. 2019, Alyousef *et al*. 2020, Feng *et al*. 2020, Lv and Kumar 2020, Roy *et al*. 2020, Xu *et al*. 2020, Zhang *et al*. 2020h, i). The first effort to examine the crack effect in the cutoff wall was conducted by Marsal and Reséndiz (1971). An analytical equation was introduced by them to calculate the seepage through an opening or a defected area in a concrete wall or a sheet pile. Researchers have studied the cutoff wall performance after being subjected to cracks and evaluated the result of the infection of barrier elements in the DF (Rice and Duncan 2009). Concrete has different applications and can be employed to build bridges, buildings, dams, pavements, highways and so on (Ni *et al*. 2019b, Cao *et al*. 2020a, Huang *et al*. 2020d, Qian *et al*. 2020b, Wu *et al*. 2020a, Yu *et al*. 2020b, Zhang *et al*. 2020e, f). Hence, it is cast in various types such as previous, green, self-consolidating and high strength concrete (Hamidian *et al*. 2011, Mohammadhassani *et al*. 2014a, b, Shariati *et al*. 2014b, Toghroli *et al*. 2017, 2018, Ziaei-Nia *et al*. 2018, Dinh-Cong *et al*. 2019, Li *et al*. 2019a, Trung *et al*. 2019b). The properties of concrete are improved using numerous methods such as cementitious replacement, fiber inclusion and surface protection (Sinaei *et al*. 2011, Shariati *et al*. 2019c, Xie *et al*. 2019, Afshar *et al*. 2020, Alaskar *et al*. 2020a, Naghipour *et al*. 2020, Shariati *et al*. 2020e, Toghroli *et al*. 2020). During the service life of building structures, several factors affect the behavior of concrete. Environmental loads such as seismic loads have a considerable impact on the properties of structural components (Ghassemieh and Bahadori 2015, Bahadori and Ghassemieh 2016, Mou and Bai 2018, Mou *et al*. 2019a, b, Zhang *et al*. 2019a, Alam *et al*. 2020a, b, c, Cao *et al*. 2020c, f, Huang *et al*. 2020a, Pang *et al*. 2020) and the dynamic response of structures have been investigated extensively (Fanaie and Ezzatshoar 2014, Fanaie *et al*. 2015, 2016, Al Kajbaf *et al*. 2018, Zhang *et al*. 2019b, Asadolahi and Fanaie 2020, Liu *et al*. 2020a, b, c). Besides, various environmental exposures can decrease the durability of concrete and other cement-based materials (Abedini *et al*. 2020b, Bao *et al*. 2020a, Hu *et al*. 2020, Kordestani *et al*. 2020, Wang *et al*. 2020a, e, Yu *et al*. 2020a, Zhang *et al*. 2020c, Zhao *et al*. 2020). The permeability effect on concrete has been evaluated in several papers. In an experimental study, the influence of various parameters such as sample thickness, the material type and the average width of the crack on the permeability of concrete was examined. It was found that the permeability is highly affected by material type and crack parameters, except for the thickness factor which had a minor effect (Aldea *et al*. 1999). Concrete is subjected to different loading conditions. Therefore, in recent years, several studies have been performed to evaluate the effect of applied loads on the performance of structural elements (Shariati *et al*. 2012, 2013, 2014a, 2017, Zhu *et al*. 2018, Abedini *et al*. 2020a, Bao *et al*. 2020b, Zhang *et al*. 2020b, d, Zhang and Mousavi 2020). Also, since the permeability of concrete could be affected by higher temperatures due to the possible thermal damage, the behavior of concrete and other elements should be assessed under elevated temperatures (Shahabi *et al*. 2016, Shi *et al*. 2017, 2018, Davoodnabi *et al*. 2019, Xue *et al*. 2019, Li *et al*. 2020a, Shariati *et al*. 2020a, Yang *et al*. 2020, Yue *et al*. 2020, Zhang *et al*. 2020g). In addition, the permeability of reinforced concrete (RC) under different loading scenarios as an essential topic has attracted the researchers' attention (Fanaie *et al*. 2017, 2019, Liu *et al*. 2017, Afrazi and Rouhanifar 2019, Zhang and Liu 2019f, Cao *et al*. 2020d, Ren *et al*. 2020, Chen *et al*. 2021a, Gao *et al*. 2021a, b). Investigations on different FRCs[1] subjected to mechanical loading indicated that their water permeability has decreased compared to normal concrete (Afrazi *et al*. 2018, Chen *et al*. 2019b, Gao *et al*. 2020, Liu *et al*. 2020d, g, Huo *et al*. 2021, Jia *et al*. 2021, Zhang *et al*. 2021). This is due to the fiber ability in providing higher tortuosity and lower porosity when applied in the concrete matrix (Liu *et al*. 2015, Hannawi *et al*. 2016, Deng *et al*. 2019, Qi and Fourie 2019, Fu *et al*. 2020, Liu *et al*. 2020e, i, Bai *et al*. 2021). Rapoport *et al*. (2002) studied the permeability of cracked steel FRC. The decrease in permeability of cracked concrete was seen by applying steel fibers at larger crack width. It was also demonstrated that the permeability of unreinforced concrete was higher than of reinforced concrete. Moreover, for smaller cracks (below 100 μm), the effect of fibers on permeability was not found. The water permeability assessment (Li *et al*. 2020d), as well as the uniaxial tensile loading test, were performed on different types of RC prisms such as HPC[2], HPFRC[3] and UHPFRC[4]. Results showed that the addition of fibers in concrete leads to decreasing water permeability compared to normal HPC (Hubert *et al*. 2015). In addition, the permeability of FRC and NSC[5] under static and constant tensile loadings was investigated. Compared to the NSC, the FRC specimens showed lower permeability (Desmettre and Charron 2012). The influence of permeability on the FRC and NSC specimens under constant and cyclic loadings was also examined. The obtained results indicated that under both loading conditions, the permeability of FRC was lower than that of NSC (Desmettre and Charron 2013, Chen *et al*. 2019a, Cao 2020, Chen *et al*. 2020a, d, Cheng and Liu 2020, Wang *et al*. 2020c). The addition of

[1] Fiber Reinforced Concretes
[2] High Performance Concrete
[3] High Performance Fiber Reinforced Concrete
[4] Ultra High Performance Fiber Reinforced Concrete
[5] Normal Strength Concrete

polypropylene (PP) fiber to concrete was studied in order to evaluate the plastic shrinkage cracks and permeability. It was deduced that incorporation of the fiber results in decreasing the crack width and plastic shrinkage cracks compared to plain concrete. However, it was revealed that incorporation of PP fibers in concrete increases the gas and water permeability (Islam and Gupta 2016). The concrete behavior can be evaluated by the SHM[6] systems. The detection of damages and other detrimental factors is a necessary issue to improve the mechanical properties of concrete and assess the performance of other building materials (Zhang 2014, Afrazi *et al*. 2017b, Bahri and Harrag 2018, Sun *et al*. 2018, 2019, Zhang and Wang 2019a, b, Chen *et al*. 2020c, Li *et al*. 2020b, Zhang and Wang 2020c). In order to eliminate the high cost of experimental studies and their time consuming process, several algorithms have been introduced which are more reliable than other classical numerical methods (Afrazi *et al*. 2017a, Zhang *et al*. 2018, Ding *et al*. 2019, Wu *et al*. 2019b, Cai *et al*. 2020f, Chen *et al*. 2020e, He *et al*. 2020b, Wang *et al*. 2020d, f). In this regard, different types of Artificial intelligence techniques (Shariati *et al*.) such as machine learning (Qiu *et al*. 2019, Shariati *et al*. 2019b, d, Trung *et al*. 2019a, Cao *et al*. 2020e, Chen *et al*. 2020b, Qian *et al*. 2020a), Neural Networks (Ni *et al*. 2019a, Yang *et al*. 2019, Zhang *et al*. 2019c, Cao *et al*. 2020b, Mousavi *et al*. 2020, Shariati *et al*. 2020c, Shi *et al*. 2020a, b) and also hybrid algorithms (Shariati *et al*. 2019a, 2020b, d, Safa *et al*. 2020) are employed to predict the characteristics of structural elements . Hence, using these techniques can be of great help for scholars to predict the effects of cracks on the concrete permeability instead of other old-fashioned approaches (Gao *et al*. 2016, Liu *et al*. 2016, Nguyen 2017, Che-Ngoc *et al*. 2018, Chao *et al*. 2020, Liu and Liu 2020g, Liu *et al*. 2020h, Qu *et al*. 2020, Wu *et al*. 2020b, Zhang *et al*. 2020a, Zhang 2020). In addition to the above algorithms, the finite element method has been used as one of the most practical approaches in various engineering applications such as structural analysis (Fanaie and Tahriri 2017, Al-khafaji 2019, Fanaie and Moghadam 2019, Qi *et al*. 2019, Abedini and Zhang 2020b, Alaskar *et al*. 2020b, Arif *et al*. 2020, Gholipour *et al*. 2020a, b, Zhu *et al*. 2020). Hitherto, various researches have been carried out to examine the infected area and its effect on the performance of cutoff walls in the DF. However, the information on the direct impact of cracks on the hydraulic conductivity of plastic concrete material is not available in the literature. Hence, this paper is aimed to investigate the crack effect on the permeability of plastic concrete. To this end, several specimens are prepared by blending different percentages of cement and bentonite, with constant portions of water and aggregates. Then, for each mixture design, some specimens are loaded up to determine the level of stress, until cracks appear in the specimens. By conducting the permeability test on the both intact and cracked samples, preparing under specific conditions and comparing the results, the effect of crack on the permeability of plastic concrete is determined.

[6] Structural Health Monitoring

2. Materials and methods

In order to show the impact of crack on the permeability of concrete, three different concrete types were used in this study. First concrete type was polypropylene fiber reinforced concrete which is regarded as type 1, steel fiber-reinforced concrete as type 2, and lastly normal concrete as type 3.

2.1 Materials

2.1.1 Cement

The type of cement applied to polypropylene fiber reinforced concrete was Portland Cement which has the strength class 52.5 N. Regarding the clinker ratio (95–100%) and gypsum (0–5%) in cement, the specific gravity was found to be 3.15. Considering steel fiber-reinforced concrete (type 2), ordinary type I Portland cement has been applied while using the steel fibers (0.5 mm diameter, 50 mm long). In this experiment 1003200 mm (438 in.) cylinders were used for casting the test series. About 9 months after the casting process, samples were examined. Furthermore, with regards to normal concrete (type 3), the concrete specimens had a thickness of 25 mm. During the splitting tests, samples were loaded such that they had 25, 50, 80, 100, 140, 180, 350, and 550 microns of crack opening displacement. After the unloading stage, a microscope was used to see the crack patterns in some of the specimens. Table 1 shows the mix ratio of normal concrete (type 3).

2.1.2 Superplasticizer

In polypropylene fiber reinforced concrete (type 1), retarding superplasticizer was based on liquid polycarboxylic ether. A small amount of superplasticizer was used in steel fiber-reinforced concrete (type 2).

2.1.3 Aggregate

The coarse sand in polypropylene fiber reinforced concrete (type 1) was fine aggregate, and the coarse aggregate was crushed stone chips (based on ASTM C33) plus doing sieve analysis. In case of coarse aggregates, washed graded pea gravel (9.5 mm maximum size) has been applied in steel fiber-reinforced concrete (type 2), river sand as fine aggregates.

2.1.4 Fiber

Table 2 demonstrates the proportionality of the concrete mixtures found in polypropylene fiber reinforced concrete (type 1). In polypropylene fiber reinforced concrete (type 1),

Table 1 Mix proportion of normal concrete (type 3)

Materials	Mix proportion	
	(kg/m^3)	(lb/yd^3)
Type 1 cement	344	579
Water	195	328
Pea gravel (oven dry)	1036	743
River sand	858	1444

Table 2 Concrete mix proportions on as polypropylene fiber reinforced concrete (type 1)

Mix code	W/C[1]	B/C[2]	Water (kg/m^3)	Cement (kg/m^3)	Bentonite (kg/m^3)	Sand 0~4.75 mm (kg/m^3)	Gravel 4.75~9.5 mm (kg/m^3)	Gravel 9.5~19 mm (kg/m^3)
A1	2.3	0.2	400	119	24	620	280	475
A2	2.2	0.2	400	125	29	620	280	475
A3	2.7	0.2	400	133	56	620	280	475
A4	2.1	0.2	400	142	35	620	280	475
A5	2.0	0.2	400	200	40	620	280	475
B1	3.0	0.3	400	133	40	620	280	475
B2	2.8	0.3	400	1413	43	620	280	475
B3	2.6	0.3	400	154	46	620	280	475
B4	2.4	0.3	400	167	35	620	280	475
B5	2.2	0.3	400	182	55	620	280	475
B6	2.0	0.3	400	200	60	620	280	475
C1	3.0	0.35	400	133	23	620	280	475
C2	2.8	0.36	400	143	50	620	280	475
C3	2.6	0.35	400	154	54	620	280	475
C4	2.4	0.32	400	167	55	620	280	475
C5	2.7	0.35	400	182	64	620	280	475
C6	2	0	400	200	67	620	280	475

*Superplasticizer. Polypropylene fiber reinforced concrete (type 1), steel fiber-reinforced concrete (type 2), normal concrete (type 3)

Table 3 Mix Proportions (by Weight), Steel Fibers (by Volume) in Concrete (type 2)

Mix	Cement	Water	Sand	Gravel	Super- plasticizer	Steel fiber volume
Control	1	0.45	2	2	0.006	—
Steel 0.5%	1	0.45	2	2	0.006	0.5%
Steel 1.0%	1	0.45	2	2	0.006	1.0%

concrete (type 1), a non-metallic fiber, in other words polypropylene, was added for increasing the crack resistance and reinforcement (chemical stability corrosion with high strength and high temperature resisting). The fiber volume was from 0.1% - 0.3%. Also, as shown in Table 2, concrete with a steel fiber content 0.5% (Vf50.5%) and 1% (Vf51%) was used in steel fiber-reinforced concrete (type 2).

2.2 Concrete mix proportions

In order to achieve the target slump value of 75 to 100 mm and strength value of 35 MPa within 28 days, a trial mixture was added to the polypropylene fiber reinforced concrete (type 1). By changing the superplasticizer dosage, desired workability was gained. Concrete mix design was based on ACI 211, 2009. A slump of fresh normal concrete (type 3) with the size of 3.2 cm had w/c of 0.41 (by weight). These specimens were cured within water in ambient (20°C) for 90-100 days prior to permeability and splitting tests. The compressive strength (CS) of 28-day was 45 MPa (6500 psi). Table 1 shows the concrete mix ratio of this research.

2.3 Concrete mixture, curing and casting

18 plains concrete and 72 fiber reinforced mixes were prepared (machine mixer) in polypropylene fiber reinforced concrete (type 1). Each trial consisted of 40 liters of the mixture. Right amount of fine aggregates (SSD), coarse aggregate (SSD) and cement were initially dry mixed (2 minutes) followed by adding superplasticizer and water. These fibers were later added to the solution while aiming to get an equal distribution within the concrete (4 minutes). A slump test was performed to determine the workability of concrete. 150 mm cube specimens have been applied for strength and permeability tests. Oiled molds were used to prevent adhesion of concrete and later filled with concrete using a standard rod and covered with a wet Hossain bag in ambient temperature (24 h). After removing from the molds, they were cured in freshwater (1 week), strength test (28 days) and permeability tests (28 days).

2.4 Concrete strength testing

In polypropylene fiber reinforced concrete (type 1), the strength of the split tensile was built upon EN 12390-6 (2000) and CS on EN 12390-3 (2009).

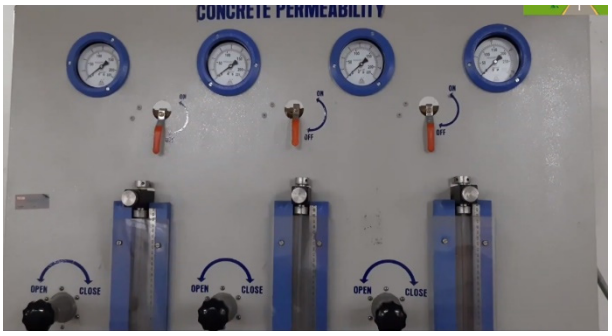

Fig. 1 Permeability water testing tool, water flowing ratio measuring inside the concrete sample

Fig. 2 Three concrete sample size

$$f_{ct} = \frac{2F}{\pi L d} \tag{1}$$

F = maximum load (*N*)
d = designated cross-sectional dimension (*mm*)
f_{ct} *= tensile splitting strength* (*MPa*)
L = line of contact of specimen's length (*mm*)

2.5 Permeability testing

Regarding polypropylene fiber reinforced concrete (type 1), the gas and water permeability tests have been conducted for fiber reinforced and plain concrete with fiber volume 0.2%, 0.25%, 0.3%. In this case, adding polypropylene fiber raises the permeability of gas and water in concrete. Plain concrete's water permeability coefficient was 5.941013 m/s after the addition of 0.2% fiber, while this number was 14.991012 m/s when the added fiber was 0.3%. Alternatively, the initial gas permeability coefficient in kg's for the plain concrete was around 47.921011 m^2. This value was increased by 60% when the added fiber was increased by 0.25%. Meaning, the gas permeability was raised as the fiber volume was raised in the mixture. In this test, minimal 0.2% fiber was taken. Following Singh and Singhal (2011) and Miloud (2005) shows that the permeability was similar by adding the steel fibers (0–0.4%) in comparison to this test with polypropylene fibers. The difference between steel fiber and other ingredients is that steel is not applicable for polypropylene fibers in concrete. In steel fiber-reinforced concrete (type 2), by the cracking of samples, they become ready for the permeability test of water. Samples were vacuumed in a vacuum jar (1 mm Hg for 3 h) based on ASTM C 1202[7] while deionized water has been added and vacuumed for extra 1 hour, then pumped off. The process followed by keeping the samples in water for extra 18 h. After saturation, every sample has been removed to the permeability test of water. Water is added to the system for permeability testing. More water was added to pipette while flowing within the concrete (out of the copper tube). The water ratio was altered inside the pipette to compute its flowing within the sample and the material's permeability. By dropping the primitive water ratio in pipette, extra water has been added. It was noted that the primary permeability was significantly greater than the final permeability. While starting the test, the specimens might not be perfectly saturated, therefore, water flowed inside the system up to reaching the permeability degree to a roughly stable level. When dealing with samples which have big cracks water should be added multiple times in the span of 24 h, instead of adding water once and waiting 24 h for it to penetrate to each specimen. The permeability coefficient of the material was calculated by taking the sample mean of 10 readings. These readings were taken when the permeability reached a constant value. The water flow through the system was kept on, then Darcy's law is used. Due to the flowing of water, the flowing ratio in pipette is

$$dV = A'\left(\frac{dh}{dt}\right) \tag{2}$$

A'= pipette's cross-section area
t = the time taken for passing a proper amount of water within the system
H = head of water formed by the water in pipette and chamber height
V = all the water rate flowed in sample

Darcy's law

$$Q = kA\frac{h}{l} \tag{3}$$

l = sample's thickness
A = concrete cross-sectional area
k = the studied parameter and permeability coefficient
Q = flowing ratio within the sample (dV/dt)

The permeability tests of water have been conducted on cracked samples when dealing with normal concrete, which also includes the test setup, specimen vacuuming and saturation, permeability measurement, and the preparation of the specimen for rapid chloride permeability tests (AASHTO T277). Samples along with the de-aired water, which was obtained from boiling deionized water for about 2 hours, were vacuumed in the water for 1 hour. This procedure was followed by putting the samples in a desiccator and soaking them for at least 12 hours.

[7] standard for the rapid chloride permeability test ASTM 1994

Fig. 3 Placing the samples that were 28 days cured and dried

Fig. 4 Removing the samples after 72 +/- 2 hours

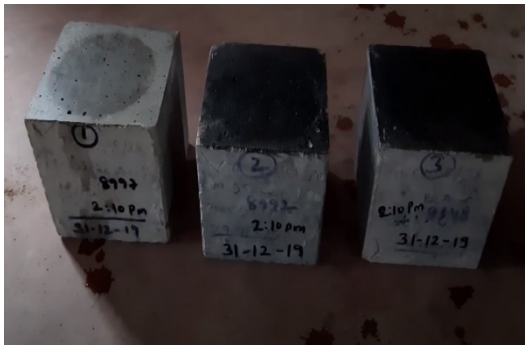

Fig. 5 Clean the water from samples

2.6 Testing process

Extraction form the desiccator: Considering the top and bottom surfaces of samples, its middle part was surfaced with a rubber disc (75 mm diameter, 1.6 mm thickness). Next, two plexiglas rings with the help of silicone rubber were placed on both top and bottom surfaces of the samples. These plexiglas rings had an inner diameter of 76 mm, thickness of 5 mm, and height of 25 mm. Afterwards, deionized water was added to cells in the below and above the samples. By filling the pipette (with water), a permeability water test was started. Water was dropped from top to bottom (300 mm of water) and regularly measured (once a day) on the basis of water flowing ratio in sample.

For every measuring the pipette was reloaded in order to keep the ratio of the water in the mixture constant. In this

Fig. 6 Immediately split the samples in the plane perpendicular to the face on which the pressure was applied

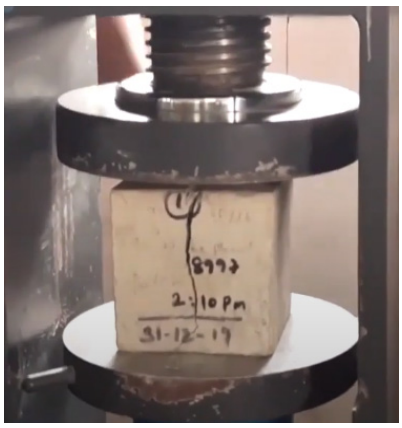

Fig. 7 The crack performed by pressure (In three concrete types)

research, the majority of samples have been tested for 20 days (few for 50 days) to be sure from the gain of the state flow. Considering the Darcy's law, permeability coefficient k (cm/set) for a falling water head is

$$\frac{dQ}{dt} = -\frac{A'dh}{dt} = k\frac{h}{L}A \tag{4}$$

$$-\frac{dh}{h} = k\frac{hA}{A'L}dt \tag{5}$$

Taking the integral from h_0 to h_1

$$k = \frac{A'L}{At}\ ln\frac{h_0}{h_1} \tag{6}$$

L = sample thickness (*cm*)
Q = water flow content (*cm*')
A = sample's cross-sectional area (*cm*')
ho = initial water heads (*cm*)
hi = final water heads (*cm*)
t = time
A' = pipette's cross sectional area (*0.5 cm*')

2.7 Splitting Tension Test (Brazilian Test)

The splitting test used in splitting normal concretes, has

Fig. 8 Measuring the water penetration and cracks

Fig. 9 Defining the crack place

Fig. 10 Measuring the crack in samples

Fig. 11 The crack in unreinforced specimen 500 µm in concrete type 2

Fig. 12 The crack size 20 mm in concrete type 1 (steel 1% specimen

a closed-loop feedback controller. Closed-loop test machines function by adjusting the actuator (loading ram) to get a desired value from a measured parameter or a feedback signal. It was the mean of measured parameters' displacement (stroke or force) through the lateral linear variable differential transducer (LVDTs) for these tests. A constant increment of the favored variables, the feedback measurement variable is raised despite decreasing the load carrying capacity of the sample. In this experiment, a cylindrical specimen (25 mm thickness, 100 mm diameter) was significantly loaded. One LVDT (0.5 mm) was firmly situated on both sides of the sample in a perpendicular fashion to the loading direction. This would make sure that the crack opening displacement (COD) is monitored. Plywood strips (3 mm thickness, 25 mm wide) were located between the loading plates and samples to avoid the

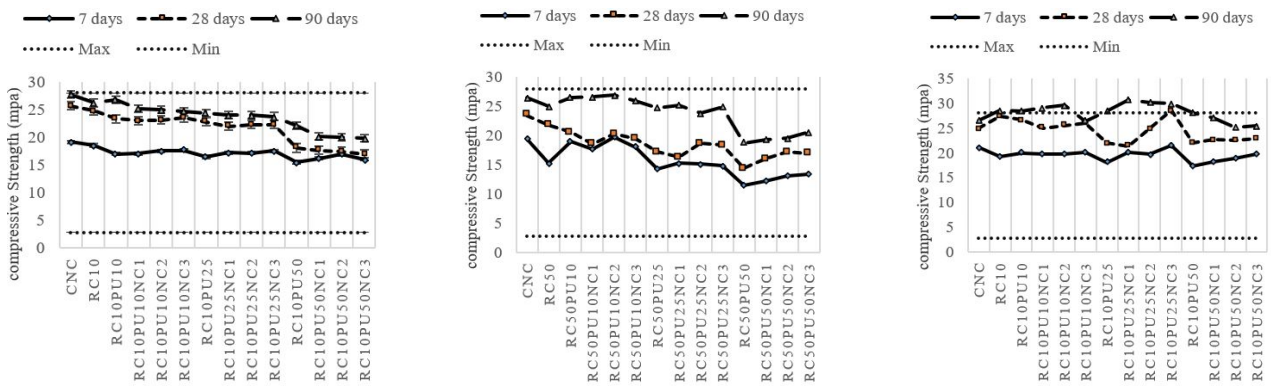

Fig. 13 The effect of adding Superplasticizer in 7, 28 and 90 days curing period on the compressive strength in polypropylene fiber reinforced concrete (type 1)

crushing at loading points. The displacement mean (average) of two LVDTs have been computed while the feedback control parameter (crack opening displacement mean) has been raised in a stable ratio of 0.2 p.m/sec. Samples were loaded to a predetermined crack width in a feedback controlled statue that later were unloaded in force control. Despite the average displacement, crack opening displacement of any LVDT, time, force and stroke have been recorded along the excrement.

3. Result and discussion

3.1 Concrete strength testing

Regarding the polypropylene fiber reinforced concrete (type 1), the average of target strength in the laboratory was 43.5 (MPa) following ACI 211 (2009). By raising the fiber volume, CS was decreased. Adding 0.3% fibers to the concrete, makes CS decrease (10%) compared to control the concrete. The combination of polypropylene fiber (0–0.4%) and steel (0.8% fixed) reduces CS after polypropylene fiber

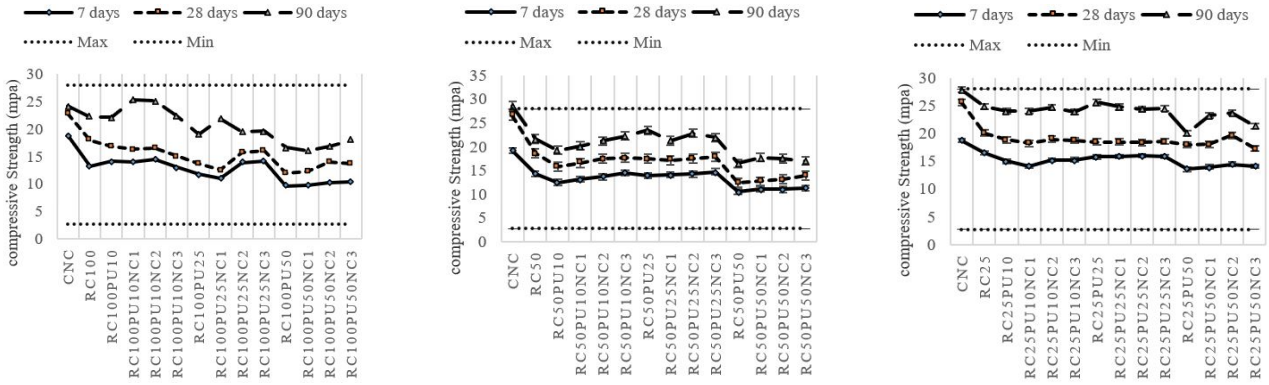

Fig. 14 The effect of adding graded pea gravel (9.5 mm maximum size) in 7, 28 and 90 days curing period on the compressive strength in steel fiber-reinforced concrete (type 2)

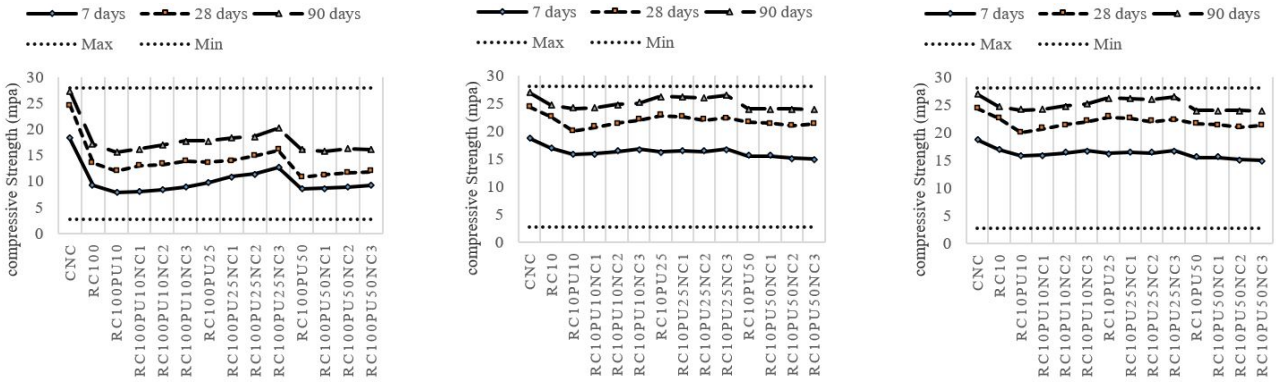

Fig. 15 The compressive strength of normal concrete (Type 3)

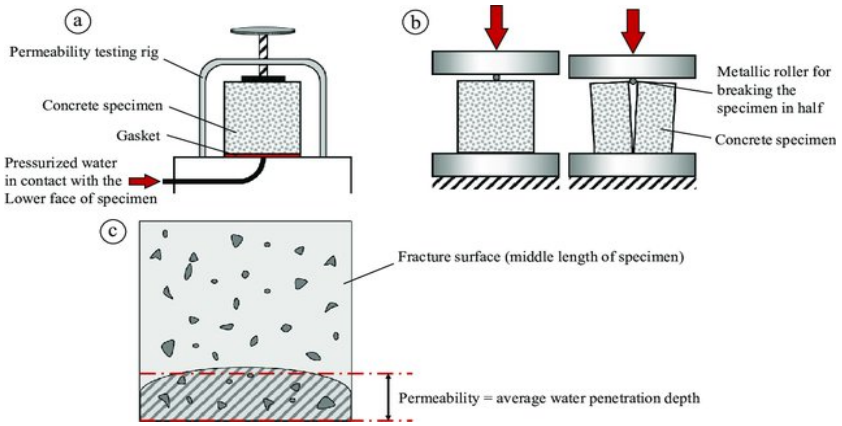

Fig. 16 Schematic design of Water permeability tool for normal concrete

content reaches a percentage higher than 0.2%. Addition of polypropylene fibers up to 0.2% alongth with 0.8% steel fiber, raised the CS value of the concrete. In steel fiber-reinforced concrete (type 2), cracks were applied to a specified crack mouth opening displacement (CMOD). Later, these cracks were relaxed while being unloaded. Every data point represents the data average of two samples. Concrete with no steel fibers (unreinforced) indicates the most crack relaxation (roughly 62%) but not in concrete with steel fibers. This result shows that the fiber-reinforced concrete has a highly inelastic (unrecoverable) deformation compared to the unreinforced one. In every experiment, the two samples were cracked to each specific CMOD, samples were tested and cracks were relaxed. After relaxation for any crack level, the ultimate CMOD was totally near to any treatment. Typically, the differential CMOD in relaxed cracks was not more than 5 mm for 100 mm cracks and 20 mm for the above 100 mm cracks. Additionally, steel fiber (1%) declines the permeability greater than 0.5% because of the multiple cracking and its stitching effect. Steel fibers can bind the cracks at the ends and decrease its length and area for permeability. 50 mm thickness size was used for cutting the samples, followed by cracking to a particular CMOD (f 100, 200, 300, 400, or 500 mm) through Splitting Tension Test. Fig. 8 shows the test tools. Splitting Tension Test compresses a circular sample making tensile stresses inside the middle of the sample that make cracks in the sample. A strain gauge extensometer (with a LVDT in maximal displacement of 1 mm or 0.5 mm) was joined to both faces of the sample to measure the width of crack(s). The displacement mean of two strain gauges or LVDTs has been considered as a feedback signal to control the cracking. On recording the cracking and loading. Cracks were induced at an opening ratio of 0.1375 m/s to the proper CMOD while recording the loading histories. While using LVDTs to induce 400 and 500 mm cracks, the strain gauges have been applied to induce cracks up to 300 mm. Later, specimens were unloaded and cracks relaxed and measured. In other words, steel fiber alters the geometry of crack from one big crack to few smaller cracks due to the distribution of stress within the material. Only the central big crack is obvious since the permeability is associated with the crack width's cube, few smaller cracks could be low permeable than one big crack. As noted, steel fibers (or more fiber) could decline the permeability of cracked concrete. Tsukamoto (1990) and Tsukamoto and Worner (1991) have tested microfiber reinforced concrete on the slopes of permeability lines, resulting in raising fiber content and reducing the permeability of cracked concrete. The tests were conducted with 95% reliability for cracks larger than 100 mm. The permeability differential is not essential with 95% reliability for cracks smaller than 100 mm.

3.2 Splitting Tension Test (Brazilian Test) or Tensile strength

The association between (type 1) and concrete tensile split strength regarded to control concrete indicated the benefits of mixing polypropylene fibers to concrete. Fibers are as the crack arrester in a concrete matrix. It was found that tensile strength was more than control (0% fiber)

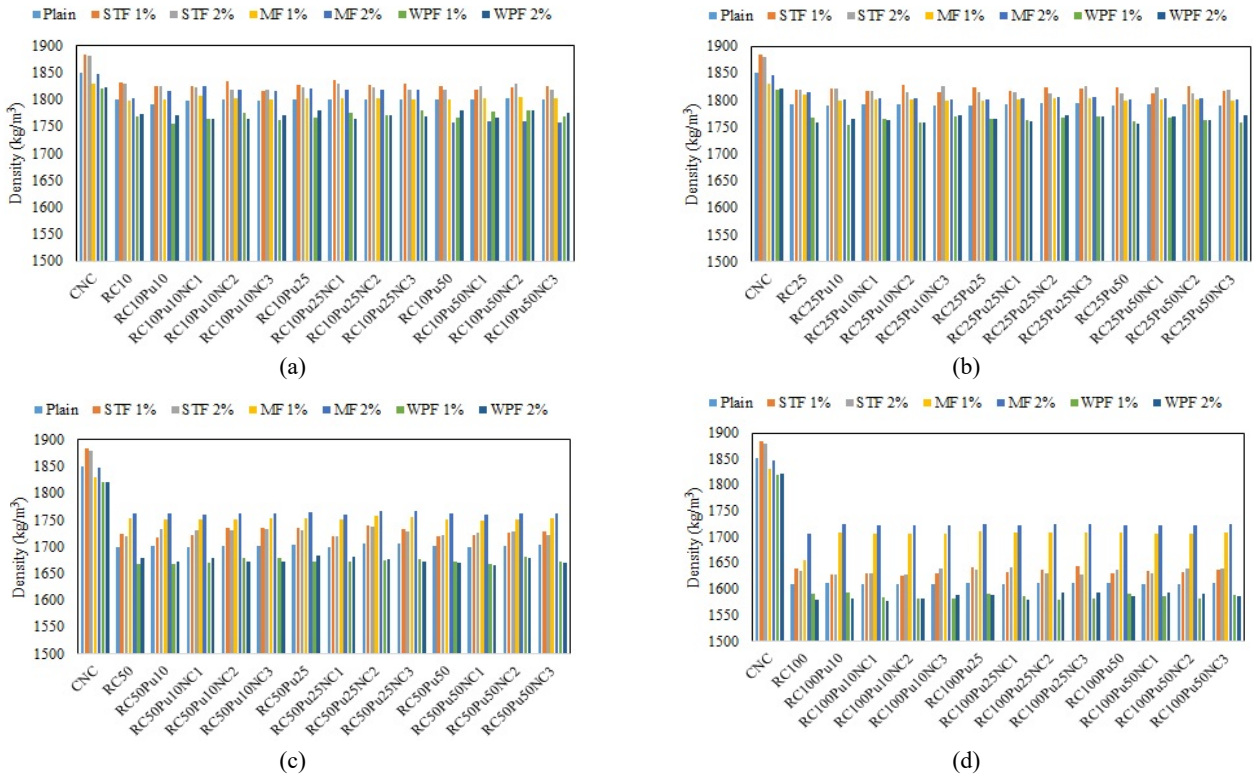

Fig. 17 The fiber volume 0.1% - 0.3%. in concrete Type 1(a, b) and steel fiber content 0.5% (Vf50.5%) and 1% (Vf51%) in concrete Type 2 (c, d)

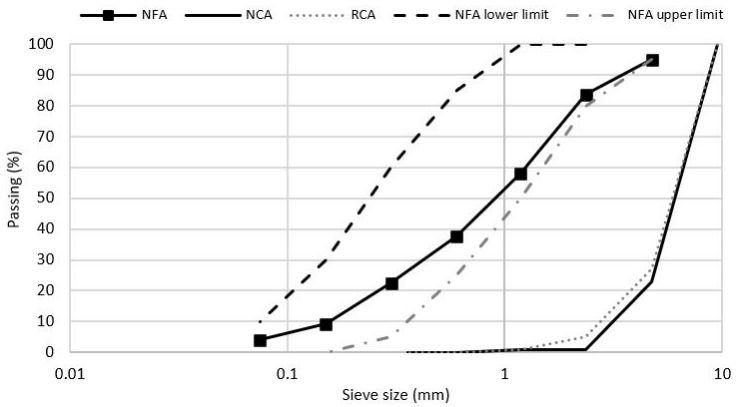

Fig. 18 Stiffness reduction in concrete due to crack opening

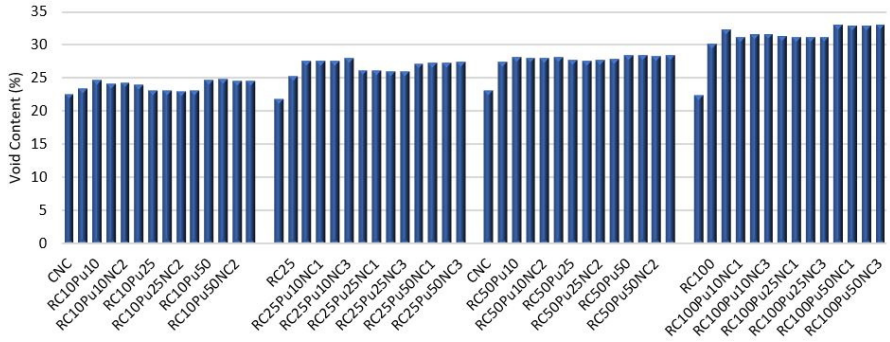

Fig. 19 Void content of concrete with polypropylene fiber reinforced concrete (type 1)

concrete with addition of 0.25% fiber and above this amount, tensile strength was less than control concrete. By adding up to 0.25% fiber, 28-day tensile strength was increased 10% to 39%. The best outcome was seen in 39% tensile splitting strength increment with 0.1% fiber addition. More fiber reduced the tensile strength while comparing with the control concrete (adding fiber 0.25%). It was noted that the combination of steel fiber 0.8% to polypropylene fiber raises the concrete's tensile strength if the addition ratio of polypropylene fibers is up to 0.3%. Tensile strength reduction also occurred. By adding the 0.3% polypropylene fiber (0.3%), strength has been raised (up to 60%), which reduced the tensile strength. In normal concrete (Type 3), the peak load happened at the transverse displacement mean (20 micron) with tensile strength of 6 MPa. The load was declined because of the advent of cracks in concrete after passing the peak stress. Typically, cracks were opened on one face and later on the other face while following the LVDTs data. Therefore, using the combination of lateral displacements measured on both faces as the feedback signal to guarantee a stable feedback control is essential. When displacement was raised, load was declined (75%) and became constant. In this study, the crack opening displacement indicates the displacement between two points in which one LVDT was amounted for all loading levels. By reaching the measured displacement to the predetermined cracked width, the sample was unloaded. There was a less steep across unloading than loading, indicating the reduction of concrete stiffness because of cracking. This reduction depended on the maximal crack opening displacement of the specimen. Based on Fig. 9, stiffness of cracked concrete was determined as a line slope joining the two points with stresses of 1 and 3 MPa in the unloading curve. After complete unloading, the crack opening displacement was declined, e.g., the crack partially was recovered or closed because of the elasticity of material. In case of unloading of the sample before reaching the peak load, roughly 80% of displacement might be recovered and the remaining crack opening displacement would be very small. Thus, crack might bring low impact on CP (as measured on unloaded samples).

3.3 Permeability tests

In normal concrete, it was found that at the initial test, the cumulative water flowing was raised nonlinearly along time, however, became constant after 3 weeks. This nonlinearity might be because of the incomplete saturation of sample and unavoidable air bubbles within the sample. The decreasing flow ratio could be because of the substances' precipitation from leaching of calcium hydroxide in concrete during the time. Substances could fill the little pores on the surface of concrete for declining permeability. Calcium hydroxide leaching occurred along the concrete specimens' curing under water. While the flow rates were essentially low, it was resulted that having a small crack, CMOD is $\leq$ than 50 microns. Accordingly, permeability readings could be once a day in the initial test week, then once in every 2 days or every 7 days to minimize

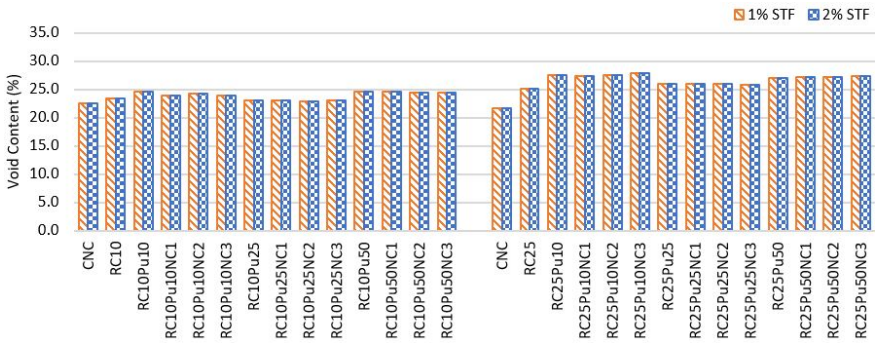

Fig. 20 Void content of concrete with steel fiber-reinforced concrete (type 2)

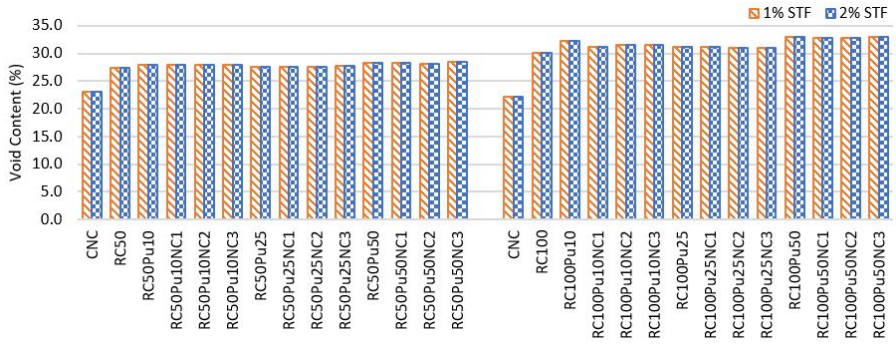

Fig. 21 Void content of concrete with normal concrete (type 3)

the reading errors. Water flowing ratio was adequately high for the specimen with a CMOD of 180 microns. Reading was done twice a day along the initial test days preventing the water dropping below the readable lever on pipette. The permeability coefficient (k) of a sample was computed through the slope of the best-fitting straight line of the last part of its permeation curve and considering the falling water head in a reading time interval. For samples with crack opening displacements of 350 and 550 microns, less than 2 minutes is required for water dropping from the top to the bottom of the pipette. Thus, the water drop time laps were recorded and the close mean of five flow ratio measurements has been applied for permeability coefficient measurement. Relationship between crack openings and water permeability was observed if the CMOD of a specimen was lower than 50 microns in loading, showing less impact of crack opening on CP. In the case of raising CMOD from 50 to 200 microns, water permeability was raised quickly. However, when the CMOD was more than 200 microns, the increasing water permeability ratio became steady. Crack length and cracks' number could affect CP beside crack width. Accurate measurements are needed for measuring the crack length including micro cracks and few cracks throughout the samples. Regarding concrete deterioration due to cracking, AC1 Building Code[8] limits crack widths by confining the flexural reinforcement distribution in reinforced concrete design. According to this research, the permeability coefficient of concrete is around 10^{-3} to 10^{-2} cm/set, when CMOD are about 300 - 400 μm compared to 10^{-10} to 10^{-9} cm/set for untracked concrete. Regarding this high permeability, considerable leaking and subsequent corrosion of reinforcement might be seen in concrete during a limited service time. Cracks generated by splitting tests might be similar in widths on the inside like the samples' surface, while the crack widths adopted by the Code are the surface crack widths and actual shear deformation of concrete cover. The curvature of flexural members would lead to narrower crack widths at the level of steel than at the surface (i.e., V-shaped cracks).

4. Conclusions

By conducting a few tests on three concrete types, this study was going to analyze the impact of crack on the permeability of these concrete types. Analyzing the test outcomes of concrete (type 1) have shown that by the rise of polypropylene content, the crack width essentially was declined (72–93% for up to 0.25% fiber) and cracks nearly vanished with 0.3% fiber addition. In case of a crack beyond the accepted domain in plain control concrete, adding fiber decreased the width of crack in the acceptable confinement (3 mm) following ACI 224 (2007). Going to the analysis of steel fiber-reinforced concrete (type 2), at larger crack widths, steel reinforcing macro-fibers declines the permeability of cracked concrete. More steel content (1%) declines the permeability more than the less steel content (0.5%) that is less than the permeability of unreinforced concrete. It could be because of crack stitching and few cracking impacts of steel fiber reinforcement. Also, the permeability differentials more than 100 mm (in all test

[8] (AC1 318-89 Commentary, Section 10.6)

series) are significant with 95% reliability. In cracks below 100 mm, steel reinforcing macro-fibers sound with no impact on the permeability of concrete. Considering the normal concrete (type 3), it was shown that 1) CMOD is recorded along the loading and after unloading 2) cracks are made by tensile stresses and 3) the cylindrical samples used in loading tests are preferable for standard CP tests. Also, the results showed that the CMOD at the peak stress is lower than 20 microns. At this loading level, about 80% of CMOD is recovered after unloading, and the remaining CMOD is highly small, indicating the little impact of cracking on CP. On the other hand, water permeability of concrete with various crack widths was measured, resulting in CP being raised with crack width. The permeability increment range depended on the crack opening value in concrete. When CMOD was less than 50 microns under loading, there was a less effect of crack opening on CP, however, by the rise of CMOD (50 to 200 microns), CP was rapidly increased. When CMOD was beyond 200 microns, the water permeability increment ratio became steady. As a result, adding polypropylene aggregate to concrete could significantly reduce the width of crack, while adding steel fiber to concrete reduces the permeability of cracked concrete compared to normal concrete that might indicate less impact of cracking on CP.

References

Abedini, M. and Zhang, C. (2020a), "Dynamic performance of concrete columns retrofitted with FRP using segment pressure technique", *Compos. Struct.*, **260**, 113473. https://doi.org/10.1016/j.compstruct.2020.113473

Abedini, M. and Zhang, C. (2020b), "Performance assessment of concrete and steel material models in ls-dyna for enhanced numerical simulation, a state of the art review", *Arch. Computat. Methods Eng.*, 1-22. https://doi.org/10.1007/s11831-020-09483-5

Abedini, M., Mutalib, A.A., Zhang, C., Mehrmashhadi, J., Raman, S.N., Alipour, R., Momeni, T. and Mussa, M.H. (2020a), "Large deflection behavior effect in reinforced concrete columns exposed to extreme dynamic loads", *Front. Struct. Civil Eng.*, **14**(2), 532-553. https://doi.org/10.1007/s11709-020-0604-9

Abedini, M., Zhang, C., Mehrmashhadi, J. and Akhlaghi, E. (2020b), "Comparison of ALE, LBE and pressure time history methods to evaluate extreme loading effects in RC column", *Structures*, **28**, 456-466. https://doi.org/10.1016/j.istruc.2020.08.084

Afrazi, M. and Rouhanifar, S. (2019), "Experimental study on mechanical behavior of sand-rubber mixtures", *Modares Civil Eng. J.*, **19**(4), 83-96.

Afrazi, M., Yazdani, M. and Fakhimi, A. (2017a), "The numerical study of effect of an oversize particle on the shear strength of sand in direct shear test", *Proceedings of the 4th International Conference on Recent Innovations in Civil Engineering, Architecture, and Urban Palnning*.

Afrazi, M., Yazdani, M. and Fakhimi, A. (2017b), "The numerical study of effect of an oversize particle on the shear strength of sand in Triaxial test", *Proceedings of the 4th International Conference on Recent Innovations in Civil Engineering, Architecture, and Urban Palnning*.

Afrazi, M., Yazdani, M., Alitalesh, M. and Fakhimi, A. (2018), "Numerical analysis of effective parameters in direct shear test by hybrid discrete – finite element method", *Modares Civil Eng. J.*, **18**(3), 13-24.

Afshar, A., Jahandari, S., Rasekh, H., Shariati, M., Afshar, A. and Shokrgozar, A. (2020), "Corrosion resistance evaluation of rebars with various primers and coatings in concrete modified with different additives", *Constr. Build. Mater.*, **262**, 120034. https://doi.org/10.1016/j.conbuildmat.2020.120034

Afsar Dizaj, E., Fanaie, N. and Zarifpour, A. (2018), "Probabilistic seismic demand assessment of steel frames braced with reduced yielding segment buckling restrained braces", *Adv. Struct. Eng.*, **21**(7), 1002-1020. https://doi.org/10.1177/1369433217737115

Al-khafaji, A. (2019), "Some Results of Differential Subordination and Differential Superordination Theorems for Univalent Functions Defined by Ruscheweyh Derivative Operator", *J. Adv. Eng. Computat.*, **3**(2). https://doi.org/10.25073/jaec.201932.237

Al Kajbaf, A., Fanaie, N. and Najarkolaie, K.F. (2018), "Numerical simulation of failure in steel posttensioned connections under cyclic loading", *Eng. Fail. Anal.*, **91**, 35-57. https://doi.org/10.1016/j.engfailanal.2018.04.024

Alam, Z., Sun, L., Zhang, C., Su, Z. and Samali, B. (2020a), "Experimental and numerical investigation on the complex behaviour of the localised seismic response in a multi-storey plan-asymmetric structure", *Struct. Infrastruct. Eng.*, **17**(1), 86-102. https://doi.org/10.1080/15732479.2020.1730914

Alam, Z., Zhang, C. and Samali, B. (2020b), "Influence of seismic incident angle on response uncertainty and structural performance of tall asymmetric structure", *Struct. Des. Tall Special Build.*, **29**(2), e1750. https://doi.org/10.1002/tal.1750

Alam, Z., Zhang, C. and Samali, B. (2020c), "The role of viscoelastic damping on retrofitting seismic performance of asymmetric reinforced concrete structures", *Earthq. Eng. Eng. Vib.*, **19**(1), 223-237. https://doi.org/10.1007/s11803-020-0558-x

Alaskar, A., Shah, S., Keerio, M.A., Phulpoto, J.A., Baharom, S., Assilzadeh, H., Alyousef, R., Alabduljabbar, H. and Mohamed, A.M. (2020a), "Development of Pozzolanic material from clay", *Adv. Concrete Constr., Int. J.*, **10**(4), 301-310. https://doi.org/10.12989/acc.2020.10.4.301

Alaskar, A., Wakil, K., Alyousef, R., Jermsittiparsert, K., Ho, L. S., Alabduljabbar, H., Alrshoudi, F. and Mohamed, A.M. (2020b), "Computational analysis of three dimensional steel frame structures through different stiffening members", *Steel Compos. Struct., Int. J.*, **35**(2), 187-197. https://doi.org/10.12989/scs.2020.35.2.187

Aldea, C.-M., Shah, S.P. and Karr, A. (1999), "Permeability of cracked concrete", *Mater. Struct.*, **32**(5), 370-376. https://doi.org/10.1007/BF02479629

Alyousef, R., Alabduljabbar, H., Mohamed, A.M., Alaskar, A., Jermsittiparsert, K. and Ho, L.S. (2020), "A model to develop the porosity of concrete as important mechanical property", *Smart Struct. Syst., Int. J.*, **26**(2), 147-156. https://doi.org/10.12989/sss.2020.26.2.147

Arif, M.Z., Ahmed, R., Sadia, U.H., Tultul, M.S.I. and Chakma, R. (2020), "Decision Tree Method Using for Fetal State Classification from Cardiotography Data", *J. Adv. Eng. Computat.*, **4**(1). https://doi.org/10.25073/jaec.202041.273

Asadolahi, S.M. and Fanaie, N. (2020), "Performance of self-centering steel moment frame considering stress relaxation in prestressed cables", *Adv. Struct. Eng.*, 1369433219900940. https://doi.org/10.1177/1369433219900940

Bahadori, A. and Ghassemieh, M. (2016), "Seismic evaluation of I-shaped beam to box-column connections with top and seat plates by the component method."

Bahri, H. and Harrag, A. (2018), "Variable Step Size P&O MPPT Controller to Improve Static and Dynamic PV System Performances", *J. Adv. Eng. Computat.*, **2**(2).

https://doi.org/10.25073/jaec.201822.94

Bai, B., Guo, Z., Zhou, C., Zhang, W. and Zhang, J. (2021), "Application of adaptive reliability importance sampling-based extended domain PSO on single mode failure in reliability engineering", *Inform. Sci.*, **546**, 42-59. https://doi.org/10.1016/j.ins.2020.07.069

Bao, J., Li, S., Zhang, P., Xue, S., Cui, Y. and Zhao, T. (2020a), "Influence of exposure environments and moisture content on water repellency of surface impregnation of cement-based materials", *J. Mater. Res. Technol.*, **9**(6), 12115-12125. https://doi.org/10.1016/j.jmrt.2020.08.046

Bao, J., Xue, S., Zhang, P., Dai, Z. and Cui, Y. (2020b), "Coupled effects of sustained compressive loading and freeze–thaw cycles on water penetration into concrete", *Struct. Concrete*, **22**, E944-E954. https://doi.org/10.1002/suco.201900200

Cai, C., Wu, X., Liu, W., Zhu, W., Chen, H., Qiu, J.C.D., Sun, C.-N., Liu, J., Wei, Q. and Shi, Y. (2020), "Selective laser melting of near-α titanium alloy Ti-6Al-2Zr-1Mo-1V: Parameter optimization, heat treatment and mechanical performance", *J. Mater. Sci. Technol.*, **57**, 51-64. https://doi.org/10.1016/j.jmst.2020.05.004

Cao, L. (2020), "Changing Port Governance Model: Port Spatial Structure and Trade Efficiency", *J. Coastal Res.*, **95**(SI), 963-968. https://doi.org/10.2112/SI95-187.1

Cao, B., Dong, W., Lv, Z., Gu, Y., Singh, S. and Kumar, P. (2020a), "Hybrid microgrid many-objective sizing optimization with fuzzy decision", *IEEE Transact. Fuzzy Syst.*, **28**(11), 2702-2710. https://doi.org/100.1109/TFUZZ.2020.3026140

Cao, B., Zhao, J., Lv, Z., Gu, Y., Yang, P. and Halgamuge, S.K. (2020b), "Multiobjective Evolution of Fuzzy Rough Neural Network via Distributed Parallelism for Stock Prediction", *IEEE Transact. Fuzzy Syst.*, **28**(5), 939-952. https://doi.org/10.1109/TFUZZ.2020.2972207

Cao, Y., Alyousef, R., Baharom, S., Shah, S., Alaskar, A., Alabduljabbar, H., Mustafa Mohamed, A. and Assilzadeh, H. (2020c), "Dynamic attainment of mixed aspect ratio for concrete members reinforced with steel fiber under impact loading", *Mech. Adv. Mater. Struct.*, 1-10. https://doi.org/10.1080/15376494.2020.1847371

Cao, Y., Fan, Q., Azar, S.M., Alyousef, R., Yousif, S.T., Wakil, K., Jermsittiparsert, K., Ho, L.S., Alabduljabbar, H. and Alaskar, A. (2020d), "Computational parameter identification of strongest influence on the shear resistance of reinforced concrete beams by fiber reinforcement polymer", *Structures*, **27**, 118-127. https://doi.org/10.1016/j.istruc.2020.05.031

Cao, Y., Wakil, K., Alyousef, R., Jermsittiparsert, K., Ho, L.S., Alabduljabbar, H., Alaskar, A., Alrshoudi, F. and Mohamed, A.M. (2020e), "Application of extreme learning machine in behavior of beam to column connections", *Structures*, **25**, 861-867. https://doi.org/10.1016/j.istruc.2020.03.058

Cao, Y., Wakil, K., Alyousef, R., Yousif, S.T., Jermsittiparsert, K., Ho, L.S., Alabduljabbar, H., Alaskar, A., Alrshoudi, F. and Mohamed, A.M. (2020f), "Computational earthquake performance of plan-irregular shear wall structures subjected to different earthquake shock situations", *Earthq. Struct., Int. J.*, **18**(5), 567-580. https://doi.org/10.12989/eas.2020.18.5.567

Chao, M., Kai, C. and Zhiwei, Z. (2020), "Research on tobacco foreign body detection device based on machine vision", *Transact. Inst. Measure. Control*, **42**(15), 2857-2871. https://doi.org/10.1177/0142331220929816

Che-Ngoc, H., Pham-Chau, A.-T. and Bora, D.J. (2018), "A New Fuzzy Rule Based Contrast Enhancement Method using The Two-Steps Automatic Clustering Algorithm", *J. Adv. Eng. Computat.*, **2**(4), 239-250. http://dx.doi.org/10.25073/jaec.201824.214

Chen, Y., He, L., Guan, Y., Lu, H. and Li, J. (2017), "Life cycle assessment of greenhouse gas emissions and water-energy optimization for shale gas supply chain planning based on multi-level approach: Case study in Barnett, Marcellus, Fayetteville, and Haynesville shales", *Energy Convers. Manage.*, **134**, 382-398. https://doi.org/10.1016/j.enconman.2016.12.019

Chen, Y., He, L., Li, J. and Zhang, S. (2018), "Multi-criteria design of shale-gas-water supply chains and production systems towards optimal life cycle economics and greenhouse gas emissions under uncertainty", *Comput. Chem. Eng.*, **109**, 216-235. https://doi.org/10.1016/j.compchemeng.2017.11.014

Chen, H., Qiao, H., Xu, L., Feng, Q. and Cai, K. (2019a), "A fuzzy optimization strategy for the implementation of RBF LSSVR model in vis–NIR analysis of pomelo maturity", *IEEE Transact. Indust. Inform.*, **15**(11), 5971-5979. https://doi.org/10.1109/TII.2019.2933582

Chen, X., Wang, D., Wang, T., Yang, Z., Zou, X., Wang, P., Luo, W., Li, Q., Liao, L. and Hu, W. (2019b), "Enhanced photoresponsivity of a GaAs nanowire metal-semiconductor-metal photodetector by adjusting the fermi level", *ACS Appl. Mater. Interf.*, **11**(36), 33188-33193. https://doi.org/10.1021/acsami.9b07891

Chen, C., Wang, X., Wang, Y., Yang, D., Yao, F., Zhang, W., Wang, B., Sewvandi, G.A., Yang, D. and Hu, D. (2020a), "Additive Manufacturing of Piezoelectric Materials", *Adv. Function. Mater.*, **30**(52), 2005141. https://doi.org/10.1002/adfm.202005141

Chen, H., Chen, A., Xu, L., Xie, H., Qiao, H., Lin, Q. and Cai, K. (2020b), "A deep learning CNN architecture applied in smart near-infrared analysis of water pollution for agricultural irrigation resources", *Agricul. Water Manage.*, **240**, 106303. https://doi.org/10.1016/j.agwat.2020.106303

Chen, H., Zhang, G., Fan, D., Fang, L. and Huang, L. (2020c), "Nonlinear lamb wave analysis for microdefect identification in mechanical structural health assessment", *Measurement*, 108026. https://doi.org/10.1016/j.measurement.2020.108026

Chen, J., Liu, G. and Liu, Y. (2020d), "Lightweight privacy-preserving raw data publishing scheme", *IEEE Transact. Emerg. Topics Comput.* https://doi.org/10.1109/TETC.2020.2974183

Chen, Z., Wang, J., Ma, K., Huang, X. and Wang, T. (2020e), "Fuzzy adaptive two-bits-triggered control for nonlinear uncertain system with input saturation and output constraint", *Int. J. Adapt. Control Signal Process.*, **34**(4), 543-559. https://doi.org/10.1002/acs.3098

Chen, F., Zhong, Y., Gao, X., Jin, Z., Wang, E., Zhu, F., Shao, X. and He, X. (2021a), "Non-uniform model of relationship between surface strain and rust expansion force of reinforced concrete."

Chen, Y., Li, J., Lu, H. and Yan, P. (2021b), "Coupling system dynamics analysis and risk aversion programming for optimizing the mixed noise-driven shale gas-water supply chains", *J. Cleaner Product.*, **278**, 123209. https://doi.org/10.1016/j.jclepro.2020.123209

Cheng, H. and Liu, Y. (2020), "An improved RSU-based authentication scheme for VANET", *J. Internet Technol.*, **21**(4), 1137-1150.

Cheng, X., He, L., Lu, H., Chen, Y. and Ren, L. (2016), "Optimal water resources management and system benefit for the Marcellus shale-gas reservoir in Pennsylvania and West Virginia", *J. Hydrol.*, **540**, 412-422. https://doi.org/10.1016/j.jhydrol.2016.06.041

Davoodnabi, S.M., Mirhosseini, S.M. and Shariati, M. (2019), "Behavior of steel-concrete composite beam using angle shear connectors at fire condition", *Steel Compos. Struct., Int. J.*, **30**(2), 141-147. https://doi.org/10.12989/scs.2019.30.2.141

Deng, Y., Zhang, T., Sharma, B.K. and Nie, H. (2019), "Optimization and mechanism studies on cell disruption and phosphorus recovery from microalgae with magnesium

modified hydrochar in assisted hydrothermal system", *Sci. Total Environ.*, **646**, 1140-1154. https://doi.org/10.1016/j.scitotenv.2018.07.369

Desmettre, C. and Charron, J.-P. (2012), "Water permeability of reinforced concrete with and without fiber subjected to static and constant tensile loading", *Cement Concrete Res.*, **42**(7), 945-952. https://doi.org/10.1016/j.cemconres.2012.03.014

Desmettre, C. and Charron, J.-P. (2013), "Water Permeability of Reinforced Concrete Subjected to Cyclic Tensile Loading", *ACI Mater. J.*, **110**(1).

Ding, L., Li, S., Gao, H., Liu, Y.-J., Huang, L. and Deng, Z. (2019), "Adaptive neural network-based finite-time online optimal tracking control of the nonlinear system with dead zone", *IEEE Transact. Cybernet*, **51**(1), 382-392. https://doi.org/10.1109/TCYB.2019.2939424

Dinh-Cong, D., Keykhosravi, M.H., Alyousef, R., Salih, M.N., Nguyen, H., Alabduljabbar, H., Alaskar, A., Alrshoudi, F. and Poi-Ngian, S. (2019), "The effect of wollastonite powder with pozzolan micro silica in conventional concrete containing recycled aggregate", *Smart Struct. Syst., Int. J.*, **24**(4), 541-552. https://doi.org/10.12989/sss.2019.24.4.541

Fanaie, N. and Ezzatshoar, S. (2014), "Studying the seismic behavior of gate braced frames by incremental dynamic analysis (IDA)", *J. Constr. Steel Res.*, **99**, 111-120. https://doi.org/10.1016/j.jcsr.2014.04.008

Fanaie, N. and Moghadam, H.S. (2019), "Experimental study of rigid connection of drilled beam to CFT column with external stiffeners", *J. Constr. Steel Res.*, **153**, 209-221. https://doi.org/10.1016/j.jcsr.2018.10.016

Fanaie, N. and Tahriri, M. (2017), "Stability and stiffness analysis of a steel frame with an oblique beam using method of least work", *J. Constr. Steel Res.*, **137**, 342-357. https://doi.org/10.1016/j.jcsr.2017.06.032

Fanaie, N., Esfahani, F.G. and Soroushnia, S. (2015), "Analytical study of composite beams with different arrangements of channel shear connectors", *Steel Compos. Struct., Int. J.*, **19**(2), 485-501. https://doi.org/10.12989/scs.2015.19.2.485

Fanaie, N., Aghajani, S. and Afsar Dizaj, E. (2016), "Strengthening of moment-resisting frame using cable–cylinder bracing", *Adv. Struct. Eng.*, **19**(11), 1736-1754. https://doi.org/10.1177/1369433216649382

Fanaie, N., Kazerani, S. and Soroushnia, S. (2017), "Numerical study of slotted web drilled flange moment frame connection", *Int. J. Numer. Methods Civil Eng.*, **1**(3), 16-23. https://doi.org/10.29252/nmce.1.3.16

Fanaie, N., Faegh, S.S. and Partovi, F. (2019), "An improved and innovative formulation for calculating amplified elastic story drift induced by RBS connections in steel moment frames", *J. Constr. Steel Res.*, **160**, 510-527. https://doi.org/10.1016/j.jcsr.2019.06.003

Feng, Q., Li, Y., Wang, N., Hao, Y., Chang, J., Wang, Z., Zhang, X., Zhang, Z. and Wang, L. (2020), "A biomimetic nanogenerator of reactive nitrogen species based on battlefield transfer strategy for enhanced immunotherapy", *Small*, **16**(25), 2002138. https://doi.org/10.1002/smll.202002138

Fu, X., Pace, P., Aloi, G., Yang, L. and Fortino, G. (2020), "Topology optimization against cascading failures on wireless sensor networks using a memetic algorithm", *Computer Networks*, **177**, 107327. https://doi.org/10.1016/j.comnet.2020.107327

Gao, N. and Lu, K. (2020), "An underwater metamaterial for broadband acoustic absorption at low frequency", *Appl. Acoust.*, **169**, 107500. https://doi.org/10.1016/j.apacoust.2020.107500

Gao, N. and Zhang, Y. (2019), "A low frequency underwater metastructure composed by helix metal and viscoelastic damping rubber", *J. Vib. Control*, **25**(3), 538-548. https://doi.org/10.1177/1077546318788446

Gao, N., Wu, J.H., Yu, L. and Hou, H. (2016), "Ultralow frequency acoustic bandgap and vibration energy recovery in tetragonal folding beam phononic crystal", *Int. J. Modern Phys. B*, **30**(18), 1650111. https://doi.org/10.1142/S0217979216501113

Gao, N., Luo, D., Cheng, B. and Hou, H. (2020), "Teaching-learning-based optimization of a composite metastructure in the 0–10 kHz broadband sound absorption range", *J. Acoust. Soc. Am.*, **148**(2), EL125-EL129. https://doi.org/10.1121/10.0001678

Gao, N., Guo, X., Deng, J., Cheng, B. and Hou, H. (2021a), "Elastic wave modulation of double-leaf ABH beam embedded mass oscillator", *Appl. Acoust.*, **173**, 107694. https://doi.org/10.1016/j.apacoust.2020.107694

Gao, N., Wang, B., Lu, K. and Hou, H. (2021b), "Complex band structure and evanescent Bloch wave propagation of periodic nested acoustic black hole phononic structure", *Appl. Acoust.*, **177**, 107906. https://doi.org/10.1016/j.apacoust.2020.107906

Ghassemieh, M. and Bahadori, A. (2015), "Seismic evaluation of a steel moment frame with cover plate connection considering flexibility by component method", *Proceedings of the 2015 world congress on Advances in Structural Engineering and Mechanics*, Incheon, Korea.

Gholipour, G., Zhang, C. and Mousavi, A.A. (2020a), "Nonlinear numerical analysis and progressive damage assessment of a cable-stayed bridge pier subjected to ship collision", *Marine Struct.*, **69**, 102662. https://doi.org/10.1016/j.marstruc.2019.102662

Gholipour, G., Zhang, C. and Mousavi, A.A. (2020b), "Numerical analysis of axially loaded RC columns subjected to the combination of impact and blast loads", *Eng. Struct.*, **219**, 110924. https://doi.org/10.1016/j.engstruct.2020.110924

Guan, Z., Xing, Q., Xu, M., Yang, R., Liu, T. and Wang, Z. (2019), "MFQE 2.0: A new approach for multi-frame quality enhancement on compressed video", *IEEE Transact. Pattern Anal. Mach. Intell.*, **43**(3), 949-963. https://doi.org/10.1109/TPAMI.2019.2944806

Hamidian, M., Shariati, M., Arabnejad, M. and Sinaei, H. (2011), "Assessment of high strength and light weight aggregate concrete properties using ultrasonic pulse velocity technique", *Int. J. Phys. Sci.*, **6**(22), 5261-5266. https://doi.org/10.5897/IJPS11.1081

Han, X., Chen, N., Yan, J., Liu, J., Liu, M. and Karellas, S. (2019), "Thermodynamic analysis and life cycle assessment of supercritical pulverized coal-fired power plant integrated with No. 0 feedwater pre-heater under partial loads", *J. Cleaner Product.*, **233**, 1106-1122. https://doi.org/10.1016/j.jclepro.2019.06.159

Han, X., Zhang, D., Yan, J., Zhao, S. and Liu, J. (2020), "Process development of flue gas desulphurization wastewater treatment in coal-fired power plants towards Zero Liquid Discharge: Energetic, economic and environmental analyses", *J. Cleaner Product.*, **261**, 121144. https://doi.org/10.1016/j.jclepro.2020.121144

Hannawi, K., Bian, H., Prince-Agbodjan, W. and Raghavan, B. (2016), "Effect of different types of fibers on the microstructure and the mechanical behavior of ultra-high performance fiber-reinforced concretes", *Compos. Part B: Eng.*, **86**, 214-220. https://doi.org/10.1016/j.compositesb.2015.09.059

He, L., Chen, Y. and Li, J. (2018a), "A three-level framework for balancing the tradeoffs among the energy, water, and air-emission implications within the life-cycle shale gas supply chains", *Resour. Conserv. Recycl.*, **133**, 206-228. https://doi.org/10.1016/j.resconrec.2018.02.015

He, L., Chen, Y., Zhao, H., Tian, P., Xue, Y. and Chen, L. (2018b), "Game-based analysis of energy-water nexus for identifying environmental impacts during Shale gas operations under stochastic input", *Sci. Total Environ.*, **627**, 1585-1601. https://doi.org/10.1016/j.scitotenv.2018.02.004

He, L., Shao, F. and Ren, L. (2020a), "Sustainability appraisal of desired contaminated groundwater remediation strategies: an information-entropy-based stochastic multi-criteria preference model", *Environ. Develop. Sustain.*, **23**, 1759-1779. https://doi.org/10.1007/s10668-020-00650-z

He, S., Guo, F. and Zou, Q. (2020b), "MRMD2. 0: A Python Tool for Machine Learning with Feature Ranking and Reduction", *Current Bioinform.*, **15**(10), 1213-1221. https://doi.org/10.2174/1574893615999200503030350

Hinchberger, S., Weck, J. and Newson, T. (2010), "Mechanical and hydraulic characterization of plastic concrete for seepage cut-off walls", *Can. Geotech. J.*, **47**(4), 461-471. https://doi.org/10.1139/T09-103

Hu, Y., Chen, Q., Feng, S. and Zuo, C. (2020), "Microscopic fringe projection profilometry: A review", *Optics Lasers Eng.*, 106192. https://doi.org/10.1016/j.optlaseng.2020.106192

Huang, H., Huang, M., Zhang, W., Pospisil, S. and Wu, T. (2020a), "Experimental Investigation on Rehabilitation of Corroded RC Columns with BSP and HPFL under Combined Loadings", *J. Struct. Eng.*, **146**(8), 04020157. https://doi.org/10.1061/(ASCE)ST.1943-541X.0002725

Huang, J., Alyousef, R., Suhatril, M., Baharom, S., Alabduljabbar, H., Alaskar, A. and Assilzadeh, H. (2020b), "Influence of porosity and cement grade on concrete mechanical properties", *Adv. Concrete Constr., Int. J.*, **10**(5), 393-402. https://doi.org/10.12989/acc.2020.10.5.393

Huang, Y., Wang, J., Wang, F. and He, B. (2020c), "Event-triggered adaptive finite-time tracking control for full state constraints nonlinear systems with parameter uncertainties and given transient performance", *ISA Transactions*, **108**, 131-143. https://doi.org/10.1016/j.isatra.2020.08.022

Huang, Z., Zheng, H., Guo, L. and Mo, D. (2020d), "Influence of the position of artificial boundary on computation accuracy of conjugated infinite element for a finite length cylindrical shell", *Acoust. Australia*, **48**(2), 287-294. https://doi.org/10.1007/s40857-020-00175-5

Hubert, M., Desmettre, C. and Charron, J.-P. (2015), "Influence of fiber content and reinforcement ratio on the water permeability of reinforced concrete", *Mater. Struct.*, **48**(9), 2795-2807. https://doi.org/10.1617/s11527-014-0354-z

Huo, S.-Y., Huang, H.-B., Wang, L.-J. and Chen, J.-J. (2021), "Deterministic interface modes in two-dimensional acoustic systems", *Int. J. Modern Phys. B*, **35**(1), 2150010. https://doi.org/10.1142/S0217979221500107

ICOLD (1985), *Filling Materials*: *For Watertight Cut Off Walls*, CIGB/ICOLD.

Islam, G.S. and Gupta, S.D. (2016), "Evaluating plastic shrinkage and permeability of polypropylene fiber reinforced concrete", *Int. J. Sustain. Built Environ.*, **5**(2), 345-354. https://doi.org/10.1016/j.ijsbe.2016.05.007

Jia, L.-C., Jin, Y.-F., Ren, J.-W., Zhao, L.-H., Yan, D.-X. and Li, Z.-M. (2021), "Highly thermally conductive liquid metal-based composites with superior thermostability for thermal management", *J. Mater. Chem. C*, **9**(8), 2904-2911. https://doi.org/10.1039/D0TC05493C

Jiang, Q., Shao, F., Gao, W., Chen, Z., Jiang, G. and Ho, Y.-S. (2018), "Unified no-reference quality assessment of singly and multiply distorted stereoscopic images", *IEEE Transact. Image Process.*, **28**(4), 1866-1881. https://doi.org/10.1109/TIP.2018.2881828

Jiao, S.-q., Jiao, H.-d., Song, W.-l., Wang, M.-y. and Tu, J.-g. (2020a), "A review on liquid metals as cathodes for molten salt/oxide electrolysis", *Int. J. Minerals Metall. Mater.*, **27**, 1588-1598. https://doi.org/10.1007/s12613-020-1971-x

Jiao, S.-q., Wang, M.-y. and Song, W.-l. (2020b), "Editorial for special issue on high-temperature molten salt chemistry and technology", *Int. J. Minerals Metall. Mater.*, **27**(12), 1569-1571.

Ju, Y., Shen, T. and Wang, D. (2020), "Bonding behavior between reactive powder concrete and normal strength concrete", *Constr. Build. Mater.*, **242**, 118024. https://doi.org/10.1016/j.conbuildmat.2020.118024

Kordestani, H., Zhang, C. and Shadabfar, M. (2020), "Beam damage detection under a moving load using random decrement technique and Savitzky–Golay Filter", *Sensors*, **20**(1), 243. https://doi.org/10.3390/s20010243

Li, D., Toghroli, A., Shariati, M., Sajedi, F., Bui, D.T., Kianmehr, P., Mohamad, E.T. and Khorami, M. (2019a), "Application of polymer, silica-fume and crushed rubber in the production of Pervious concrete", *Smart Struct. Syst., Int. J.*, **23**(2), 207-214. https://doi.org/10.12989/sss.2019.23.2.207

Li, T., Xu, M., Zhu, C., Yang, R., Wang, Z. and Guan, Z. (2019b), "A deep learning approach for multi-frame in-loop filter of HEVC", *IEEE Transact. Image Process.*, **28**(11), 5663-5678. https://doi.org/10.1109/TIP.2019.2921877

Li, B.-H., Liu, Y., Zhang, A.-M., Wang, W.-H. and Wan, S. (2020a), "A Survey on Blocking Technology of Entity Resolution", *J. Comput. Sci. Technol.*, **35**(4), 769-793. https://doi.org/10.1007/s11390-020-0350-4

Li, C., Sun, L., Xu, Z., Wu, X., Liang, T. and Shi, W. (2020b), "Experimental Investigation and Error Analysis of High Precision FBG Displacement Sensor for Structural Health Monitoring", *Int. J. Struct. Stabil. Dyn.*, **20**(6), 2040011. https://doi.org/10.1142/S0219455420400118

Li, X., Zhang, R., Zhang, X., Zhu, P. and Yao, T. (2020c), "Silver-Catalyzed Decarboxylative Allylation of Difluoroarylacetic Acids with Allyl Sulfones in Water", *Chem. - Asian J.*, **15**(7), 1175-1179. https://doi.org/10.1002/asia.202000059

Li, Z., Liu, H., Dun, Z., Ren, L. and Fang, J. (2020d), "Grouting effect on rock fracture using shear and seepage assessment", *Constr. Build. Mater.*, **242**, 118131. https://doi.org/10.1016/j.conbuildmat.2020.118131

Liu, L. and Liu, S. (2020), "Integrated production and distribution problem of perishable products with a minimum total order weighted delivery time", *Mathematics*, **8**(2), 146. https://doi.org/10.3390/math8020146

Liu, J., Wu, C., Wu, G. and Wang, X. (2015), "A novel differential search algorithm and applications for structure design", *Appl. Mathe. Computat.*, **268**, 246-269. https://doi.org/10.1016/j.amc.2015.06.036

Liu, S., Chan, F.T. and Ran, W. (2016), "Decision making for the selection of cloud vendor: An improved approach under group decision-making with integrated weights and objective/subjective attributes", *Expert Syst. Applicat.*, **55**, 37-47. https://doi.org/10.1016/j.eswa.2016.01.059

Liu, G., Ren, G., Zhao, L., Cheng, L., Wang, C. and Sun, B. (2017), "Antibacterial activity and mechanism of bifidocin A against Listeria monocytogenes", *Food Control*, **73**, 854-861. https://doi.org/10.1016/j.foodcont.2016.09.036

Liu, Y., Hu, B., Wu, S., Wang, M., Zhang, Z., Cui, B., He, L. and Du, M. (2019), "Hierarchical nanocomposite electrocatalyst of bimetallic zeolitic imidazolate framework and MoS2 sheets for non-Pt methanol oxidation and water splitting", *Appl. Catal. B: Environ.*, **258**, 117970. https://doi.org/10.1016/j.apcatb.2019.117970

Liu, C., Deng, X., Liu, J., Peng, T., Yang, S. and Zheng, Z. (2020a), "Dynamic response of saddle membrane structure under hail impact", *Eng. Struct.*, **214**, 110597. https://doi.org/10.1016/j.engstruct.2020.110597

Liu, C., Wang, F., Deng, X., Pang, S., Liu, J., Wu, Y. and Xu, Z. (2020b), "Hailstone-induced dynamic responses of pretensioned umbrella membrane structure", *Adv. Struct. Eng.*, 1369433220940149. https://doi.org/10.1177/1369433220940149

Liu, C., Wang, F., He, L., Deng, X., Liu, J. and Wu, Y. (2020c),

"Experimental and numerical investigation on dynamic responses of the umbrella membrane structure excited by heavy rainfall", *J. Vib. Control*, **27**(5-6). https://doi.org/10.1177/1077546320932691

Liu, C., Wu, X., Wakil, K., Jermsittiparsert, K., Ho, L.S., Alabduljabbar, H., Alaskar, A., Alrshoudi, F., Alyousef, R. and Mohamed, A.M. (2020d), "Computational estimation of the earthquake response for fibre reinforced concrete rectangular columns", *Steel Compos. Struct., Int. J.*, **34**(5), 743-767. https://doi.org/10.12989/scs.2020.34.5.743

Liu, J., Liu, Y. and Wang, X. (2020e), "An environmental assessment model of construction and demolition waste based on system dynamics: a case study in Guangzhou", *Environ. Sci. Pollut. Res.*, **27**(30), 37237-37259. https://doi.org/10.1007/s11356-019-07107-5

Liu, J., Wang, C., Sun, H., Wang, H., Rong, F., He, L., Lou, Y., Zhang, S., Zhang, Z. and Du, M. (2020f), "CoOx/CoNy nanoparticles encapsulated carbon-nitride nanosheets as an efficiently trifunctional electrocatalyst for overall water splitting and Zn-air battery", *Appl. Catal. B: Environ.*, **279**, 119407. https://doi.org/10.1016/j.apcatb.2020.119407

Liu, Q., Song, Z., Han, H., Donkor, S., Jiang, L., Wang, W. and Chu, H. (2020g), "A novel green reinforcement corrosion inhibitor extracted from waste Platanus acerifolia leaves", *Constr. Build. Mater.*, **260**, 119695. https://doi.org/10.1016/j.conbuildmat.2020.119695

Liu, S., Yu, W., Chan, F.T. and Niu, B. (2020h), "A variable weight-based hybrid approach for multi-attribute group decision making under interval-valued intuitionistic fuzzy sets", *Int. J. Intell. Syst.*, **36**(2), 1015-1052. https://doi.org/10.1002/int.22329

Liu, Y., Zhang, B., Feng, Y., Lv, X., Ji, D., Niu, Z., Yang, Y., Zhao, X. and Fan, Y. (2020i), "Development of 340-GHz Transceiver Front End Based on GaAs Monolithic Integration Technology for THz Active Imaging Array", *Appl. Sci.*, **10**(21), 7924. https://doi.org/10.3390/app10217924

Lv, Z. and Kumar, N. (2020), "Software defined solutions for sensors in 6G/IoE", *Comput. Commun.*, **153**, 42-47. https://doi.org/10.1016/j.comcom.2020.01.060

Lv, Z. and Qiao, L. (2020), "Deep belief network and linear perceptron based cognitive computing for collaborative robots", *Appl. Soft Comput.*, **92**, 106300. https://doi.org/10.1016/j.asoc.2020.106300

Lv, Z. and Song, H. (2019), "Mobile internet of things under data physical fusion technology", *IEEE Internet of Things Journal*, **7**(5), 4616-4624. https://doi.org/10.1109/JIOT.2019.2954588

Lv, Z. and Xiu, W. (2019), "Interaction of edge-cloud computing based on SDN and NFV for next generation IoT", *IEEE Internet of Things Journal*, **7**(7), 5706-5712. https://doi.org/10.1109/JIOT.2019.2942719

Mahboubi, A. and Ajorloo, A. (2005), "Experimental study of the mechanical behavior of plastic concrete in triaxial compression", *Cement Concrete Res.*, **35**(2), 412-419. https://doi.org/10.1016/j.cemconres.2004.09.011

Marsal, R.J. and Reséndiz, D. (1971), "Effectiveness of cutoffs in earth foundations and abutments of dams", *Proceedings of the Fourth Pan-American Conference on Soil Mechanics and Foundation Engineering*.

Miloud, B. (2005), "Permeability and porosity characteristics of steel fiber reinforced concrete", *Asian J. Civil Eng. (Build. Hous.)*, **6**(4), 317-330. https://www.sid.ir/en/journal/ViewPaper.aspx?id=48863

Mohammadhassani, M., Akib, S., Shariati, M., Suhatril, M. and Arabnejad Khanouki, M.M. (2014a), "An experimental study on the failure modes of high strength concrete beams with particular references to variation of the tensile reinforcement ratio", *Eng. Fail. Anal.*, **41**, 73-80. https://doi.org/10.1016/j.engfailanal.2013.08.014

Mohammadhassani, M., Suhatril, M., Shariati, M. and Ghanbari, F. (2014b), "Ductility and strength assessment of HSC beams with varying of tensile reinforcement ratios", *Struct. Eng. Mech., Int. J.*, **48**(6), 833-848. https://doi.org/10.12989/sem.2013.48.6.833

Mou, B. and Bai, Y. (2018), "Experimental investigation on shear behavior of steel beam-to-CFST column connections with irregular panel zone", *Eng. Struct.*, **168**, 487-504. https://doi.org/10.1016/j.engstruct.2018.04.029

Mou, B., Li, X., Bai, Y. and Wang, L. (2019a), "Shear behavior of panel zones in steel beam-to-column connections with unequal depth of outer annular stiffener", *J. Struct. Eng.*, **145**(2), 04018247. https://doi.org/10.1061/(ASCE)ST.1943-541X.0002256

Mou, B., Zhao, F., Qiao, Q., Wang, L., Li, H., He, B. and Hao, Z. (2019b), "Flexural behavior of beam to column joints with or without an overlying concrete slab", *Eng. Struct.*, **199**, 109616. https://doi.org/10.1016/j.engstruct.2019.109616

Mousavi, A.A., Zhang, C., Masri, S.F. and Gholipour, G. (2020), "Structural damage localization and quantification based on a ceemdan hilbert transform neural network approach: A model steel truss bridge case study", *Sensors*, **20**(5), 1271. https://doi.org/10.3390/s20051271

Naghipour, M., Niak, K.M., Shariati, M. and Toghroli, A. (2020), "Effect of progressive shear punch of a foundation on a reinforced concrete building behavior", *Steel Compos. Struct., Int. J.*, **35**(2), 279-294. https://doi.org/10.12989/scs.2020.35.2.279

Nguyen, T.B.T. (2017), "Adaptive MIMO Controller Design for Chaos Synchronization in Coupled Josephson Junctions via Fuzzy Neural Networks", *J. Adv. Eng. Computat.*, **1**(1), 80-86. http://dx.doi.org/10.25073/jaec.201711.52

Ni, T., Chang, H., Song, T., Xu, Q., Huang, Z., Liang, H., Yan, A. and Wen, X. (2019a), "Non-intrusive online distributed pulse shrinking-based interconnect testing in 2.5 D IC", *IEEE Transact. Circuits Syst. II: Express Briefs*, **67**(11), 2657-2661. https://doi.org/10.1109/TCSII.2019.2962824

Ni, T., Yao, Y., Chang, H., Lu, L., Liang, H., Yan, A., Huang, Z. and Wen, X. (2019b), "LCHR-TSV: Novel low cost and highly repairable honeycomb-based TSV redundancy architecture for clustered faults", *IEEE Transact. Comput.-Aided Des. Integr. Circuits Syst.*, **39**(10), 2938-2951. https://doi.org/10.1109/TCAD.2019.2946243

Ni, T., Xu, Q., Huang, Z., Liang, H., Yan, A. and Wen, X. (2020), "A cost-effective TSV repair architecture for clustered faults in 3D IC", *IEEE Transact. Comput.-Aided Des. Integr. Circuits Syst.* https://doi.org/10.1109/TCAD.2020.3025169

Pang, R., Xu, B., Zhou, Y., Zhang, X. and Wang, X. (2020), "Fragility analysis of high CFRDs subjected to mainshock-aftershock sequences based on plastic failure", *Eng. Struct.*, **206**, 110152. https://doi.org/10.1016/j.engstruct.2019.110152

Pisheh, Y.P. and Hosseini, S.M.M. (2012), "Stress-strain behavior of plastic concrete using monotonic triaxial compression tests", *J. Central South Univ.*, **19**(4), 1125-1131. https://doi.org/10.1007/s11771-012-1118-y

Qi, C. and Fourie, A. (2019), "Cemented paste backfill for mineral tailings management: Review and future perspectives", *Minerals Eng.*, **144**, 106025. https://doi.org/10.1016/j.mineng.2019.106025

Qi, C., Fourie, A., Chen, Q. and Liu, P. (2019), "Application of first-principles theory in ferrite phases of cemented paste backfill", *Minerals Eng.*, **133**, 47-51. https://doi.org/10.1016/j.mineng.2019.01.011

Qian, J., Feng, S., Li, Y., Tao, T., Han, J., Chen, Q. and Zuo, C. (2020a), "Single-shot absolute 3D shape measurement with deep-learning-based color fringe projection profilometry",

Optics Letters, **45**(7), 1842-1845. https://doi.org/10.1364/OL.388994

Qian, J., Feng, S., Tao, T., Hu, Y., Li, Y., Chen, Q. and Zuo, C. (2020b), "Deep-learning-enabled geometric constraints and phase unwrapping for single-shot absolute 3D shape measurement", *APL Photonics*, **5**(4), 046105. https://doi.org/10.1063/5.0003217

Qiu, T., Shi, X., Wang, J., Li, Y., Qu, S., Cheng, Q., Cui, T. and Sui, S. (2019), "Deep learning: A rapid and efficient route to automatic metasurface design", *Adv. Sci.*, **6**(12), 1900128. https://doi.org/10.1002/advs.201900128

Qu, S., Han, Y., Wu, Z. and Raza, H. (2020), "Consensus modeling with asymmetric cost based on data-driven robust optimization", *Group Decision Negotiat.*, 1-38. https://doi.org/10.1007/s10726-020-09707-w

Rapoport, J., Aldea, C.-M., Shah, S.P., Ankenman, B. and Karr, A. (2002), "Permeability of cracked steel fiber-reinforced concrete", *J. Mater. Civil Eng.*, **14**(4), 355-358. https://doi.org/10.1061/(ASCE)0899-1561(2002)14:4(355)

Ren, J., Zhang, C. and Hao, Q. (2020), "A theoretical method to evaluate honeynet potency", *Future Generat. Comput. Syst.*, **116**, 76-85. https://doi.org/10.1016/j.future.2020.08.021

Rice, J.D. and Duncan, J.M. (2009), "Findings of case histories on the long-term performance of seepage barriers in dams", *J. Geotech. Geoenviron. Eng.*, **136**(1), 2-15. https://doi.org/10.1061/(ASCE)GT.1943-5606.0000175

Roy, S.K., Nayak, D., Dash, N., Dhawan, N. and Rath, S.S. (2020), "Microwave-assisted reduction roasting—magnetic separation studies of two mineralogically different low-grade iron ores", *Int. J. Minerals Metall. Mater.*, **27**(11), 1449-1461. https://doi.org/10.1007/s12613-020-1992-5

Safa, M., Sari, P.A., Shariati, M., Suhatril, M., Trung, N.T., Wakil, K. and Khorami, M. (2020), "Development of neuro-fuzzy and neuro-bee predictive models for prediction of the safety factor of eco-protection slopes", *Physica A: Statist. Mech. Applicat.*, 124046. https://doi.org/10.1016/j.physa.2019.124046

Shahabi, S., Ramli Sulong, N.H., Shariati, M., Mohammadhassani, M. and Shah, S. (2016), "Numerical analysis of channel connectors under fire and a comparison of performance with different types of shear connectors subjected to fire", *Steel Compos. Struct., Int. J.*, **20**(3), 651-669. https://10.12989/scs.2016.20.3.651

Shariati, M., Ramli Sulong, N.H. and Arabnejad Khanouki, M.M. (2012), "Experimental assessment of channel shear connectors under monotonic and fully reversed cyclic loading in high strength concrete", *Mater. Des.*, **34**, 325-331. https://doi.org/10.1016/j.matdes.2011.08.008

Shariati, M., Ramli Sulong, N.H., Suhatril, M., Shariati, A., Arabnejad Khanouki, M.M. and Sinaei, H. (2013), "Comparison of behaviour between channel and angle shear connectors under monotonic and fully reversed cyclic loading", *Constr. Build. Mater.*, **38**, 582-593. https://doi.org/10.1016/j.conbuildmat.2012.07.050

Shariati, A., Shariati, M., Ramli Sulong, N.H., Suhatril, M., Arabnejad Khanouki, M.M. and Mahoutian, M. (2014a), "Experimental assessment of angle shear connectors under monotonic and fully reversed cyclic loading in high strength concrete", *Constr. Build. Mater.*, **52**, 276-283. http://dx.doi.org/10.1016/j.conbuildmat.2013.11.036

Shariati, M., Shariati, A., Ramli Sulong, N.H., Suhatril, M. and Arabnejad Khanouki, M.M. (2014b), "Fatigue energy dissipation and failure analysis of angle shear connectors embedded in high strength concrete", *Eng. Fail. Anal.*, **41**, 124-134. https://doi.org/10.1016/j.engfailanal.2014.02.017

Shariati, M., Toghroli, A., Jalali, A. and Ibrahim, Z. (2017), "Assessment of stiffened angle shear connector under monotonic and fully reversed cyclic loading", *Proceedings of the 5th International Conference on Advances in Civil, Structural and Mechanical Engineering-CSM 2017*.

Shariati, M., Mafipour, M.S., Mehrabi, P., Bahadori, A., Zandi, Y., Salih, M.N., Nguyen, H., Dou, J., Song, X. and Poi-Ngian, S. (2019a), "Application of a hybrid artificial neural network-particle swarm optimization (ANN-PSO) model in behavior prediction of channel shear connectors embedded in normal and high-strength concrete", *Appl. Sci.*, **9**(24), 5534. https://doi.org/10.3390/app9245534

Shariati, M., Mafipour, M.S., Mehrabi, P., Zandi, Y., Dehghani, D., bahadori, A., Shariati, A., Trung, N.T., Salih, M.N. and Poi-Ngian, S. (2019b), "Application of Extreme Learning Machine (ELM) and Genetic Programming (GP) to design steel-concrete composite floor systems at elevated temperatures", *Steel Compos. Struct., Int. J.*, **33**(3), 319-332. https://doi.org/10.12989/scs.2019.33.3.319

Shariati, M., Rafiei, S., Zandi, Y., Fooladvand, R., Gharehaghaj, B., Shariat, A., Trung, N.T., Salih, M.N., Mehrabi, P. and Poi-Ngian, S. (2019c), "Experimental investigation on the effect of cementitious materials on fresh and mechanical properties of self-consolidating concrete", *Adv. Concrete Constr., Int. J.*, **8**(3), 225-237. https://doi.org/10.12989/acc.2019.8.3.225

Shariati, M., Trung, N.-T., Wakil, K., Mehrabi, P., Safa, M. and Khorami, M. (2019d), "Moment-rotation estimation of steel rack connection using extreme learning machine", *Steel Compos. Struct., Int. J.*, **31**(5), 427-435. https://doi.org/10.12989/scs.2019.31.5.427

Shariati, M., Grayeli, M., Shariati, A. and Naghipour, M. (2020a), "Performance of composite frame consisting of steel beams and concrete filled tubes under fire loading", *Steel Compos. Struct., Int. J.*, **36**(5), 587-602. https://doi.org/10.12989/scs.2020.36.5.587

Shariati, M., Mafipour, M.S., Ghahremani, B., Azarhomayun, F., Ahmadi, M., Trung, N.T. and Shariati, A. (2020b), "A novel hybrid extreme learning machine–grey wolf optimizer (ELM-GWO) model to predict compressive strength of concrete with partial replacements for cement", *Eng. Comput.*, 1-23. https://doi.org/10.1007/s00366-020-01081-0

Shariati, M., Mafipour, M.S., Haido, J.H., Yousif, S.T., Toghroli, A., Trung, N.T. and Shariati, A. (2020c), "Identification of the most influencing parameters on the properties of corroded concrete beams using an Adaptive Neuro-Fuzzy Inference System (ANFIS)", *Steel Compos. Struct., Int. J.*, **34**(1), 155-170. https://doi.org/10.12989/scs.2020.34.1.155

Shariati, M., Mafipour, M.S., Mehrabi, P., Ahmadi, M., Wakil, K., Trung, N.T. and Toghroli, A. (2020d), "Prediction of concrete strength in presence of furnace slag and fly ash using Hybrid ANN-GA (Artificial Neural Network-Genetic Algorithm)", *Smart Struct. Syst., Int. J.*, **25**(2), 183-195. https://doi.org/10.12989/sss.2020.25.2.183

Shariati, M., Shariati, A., Trung, N.T., Shoaei, P., Ameri, F., Bahrami, N. and Zamanabadi, S.N. (2020e), "Alkali-activated slag (AAS) paste: Correlation between durability and microstructural characteristics", *Constr. Build. Mater.*, **267**, 120886. https://doi.org/10.1016/j.conbuildmat.2020.120886

Shariati, M., Mafipour, M.S., Mehrabi, P., Shariati, A., Toghroli, A., Trung, N.T. and Salih, M.N. (2020f), "A novel approach to predict shear strength of tilted angle connectors using artificial intelligence techniques", *Eng. Comput.*, 1-21. https://doi.org/10.1007/s00366-019-00930-x

Shi, K., Tang, Y., Liu, X. and Zhong, S. (2017), "Non-fragile sampled-data robust synchronization of uncertain delayed chaotic Lurie systems with randomly occurring controller gain fluctuation", *ISA Transact.*, **66**, 185-199. https://doi.org/10.1016/j.isatra.2016.11.002

Shi, K., Tang, Y., Zhong, S., Yin, C., Huang, X. and Wang, W. (2018), "Nonfragile asynchronous control for uncertain chaotic

Lurie network systems with Bernoulli stochastic process", *Int. J. Robust Nonlinear Control*, **28**(5), 1693-1714. https://doi.org/10.1002/rnc.3980

Shi, K., Wang, J., Tang, Y. and Zhong, S. (2020a), "Reliable asynchronous sampled-data filtering of T–S fuzzy uncertain delayed neural networks with stochastic switched topologies", *Fuzzy Sets Syst.*, **381**, 1-25. https://doi.org/10.1016/j.fss.2018.11.017

Shi, K., Wang, J., Zhong, S., Tang, Y. and Cheng, J. (2020b), "Non-fragile memory filtering of TS fuzzy delayed neural networks based on switched fuzzy sampled-data control", *Fuzzy Sets Syst.*, **394**, 40-64. https://doi.org/10.1016/j.fss.2019.09.001

Sinaei, H., Jumaat, M.Z. and Shariati, M. (2011), "Numerical investigation on exterior reinforced concrete Beam-Column joint strengthened by composite fiber reinforced polymer (CFRP)", *Int. J. Phys. Sci.*, **6**(28), 6572-6579. https://doi.org/10.5897/IJPS11.1225

Singh, A. and Singhal, D. (2011), "Permeability of steel fibre reinforced concrete influence of fibre parameters", *Procedia Eng.*, **14**, 2823-2829. https://doi.org/10.1016/j.proeng.2011.07.355

Soroush, A. and Soroush, M. (2005), "Parameters affecting the thickness of bentonite cake in cutoff wall construction: case study and physical modeling", *Can. Geotech. J.*, **42**(2), 646-654 https://doi.org/10.1139/t04-090

Sun, L., Li, C., Zhang, C., Su, Z. and Chen, C. (2018), "Early monitoring of rebar corrosion evolution based on FBG sensor", *Int. J. Struct. Stabil. Dyn.*, **18**(8), 1840001. https://doi.org/10.1142/S0219455418400011

Sun, L., Li, C., Zhang, C., Liang, T. and Zhao, Z. (2019), "The strain transfer mechanism of fiber bragg grating sensor for extra large strain monitoring", *Sensors*, **19**(8), 1851. https://doi.org/10.3390/s19081851

Sun, L., Yang, Z., Jin, Q. and Yan, W. (2020), "Effect of Axial Compression Ratio on Seismic Behavior of GFRP Reinforced Concrete Columns", *Int. J. Struct. Stabil. Dyn.*, **20**(6), 2040004. https://doi.org/10.1142/S0219455420400040

Toghroli, A., Shariati, M., Karim, M.R. and Ibrahim, Z. (2017), "Investigation on composite polymer and silica fume–rubber aggregate pervious concrete", *Proceedings of the 5th International Conference on Advances in Civil, Structural and Mechanical Engineering - CSM 2017*, Zurich, Switzerland.

Toghroli, A., Shariati, M., Sajedi, F., Ibrahim, Z., Koting, S., Mohamad, E.T. and Khorami, M. (2018), "A review on pavement porous concrete using recycled waste materials", *Smart Struct. Syst., Int. J.*, **22**(4), 433-440. https://doi.org/10.12989/sss.2018.22.4.433

Toghroli, A., Mehrabi, P., Shariati, M., Trung, N.T., Jahandari, S. and Rasekh, H. (2020), "Evaluating the use of recycled concrete aggregate and pozzolanic additives in fiber-reinforced pervious concrete with industrial and recycled fibers", *Constr. Build. Mater.*, **252**, 118997. https://doi.org/10.1016/j.conbuildmat.2020.118997

Trung, N.-T., Shahgoli, A.F., Zandi, Y., Shariati, M., Wakil, K., Safa, M. and Khorami, M. (2019a), "Moment-rotation prediction of precast beam-to-column connections using extreme learning machine", *Struct. Eng. Mech., Int. J.*, **70**(5), 639-647. https://doi.org/10.12989/sem.2019.70.5.639

Trung, N.T., Alemi, N., Haido, J.H., Shariati, M., Baradaran, S. and Yousif, S.T. (2019b), "Reduction of cement consumption by producing smart green concretes with natural zeolites", *Smart Struct. Syst., Int. J.*, **24**(3), 415-425. https://doi.org/10.12989/sss.2019.24.3.415

Tsai, Y.-H., Wang, J., Chien, W.-T., Wei, C.-Y., Wang, X. and Hsieh, S.-H. (2019), "A BIM-based approach for predicting corrosion under insulation", *Automat. Constr.*, **107**, 102923. https://doi.org/10.1016/j.autcon.2019.102923

Wang, W., Guo, J., Long, C., Li, W. and Guan, J. (2015), "Flaky carbonyl iron particles with both small grain size and low internal strain for broadband microwave absorption", *J. Alloys Compounds*, **637**, 106-111. https://doi.org/10.1016/j.jallcom.2015.02.220

Wang, J., Huang, Y., Wang, T., Zhang, C. and hui Liu, Y. (2020a), "Fuzzy finite-time stable compensation control for a building structural vibration system with actuator failures", *Appl. Soft Comput.*, **93**, 106372. https://doi.org/10.1016/j.asoc.2020.106372

Wang, J., Zhu, P., He, B., Deng, G., Zhang, C. and Huang, X. (2020b), "An adaptive neural sliding mode control with ESO for uncertain nonlinear systems", *Int. J. Control Automat. Syst.*, 1-11. https://doi.org/10.1007/s12555-019-0972-x

Wang, L., Huang, Y., Xie, Y. and Du, Y. (2020c), "A new regularization method for dynamic load identification", *Science Progress*, **103**(3), 0036850420931283. https://doi.org/10.1177/0036850420931283

Wang, X.-F., Gao, P., Liu, Y.-F., Li, H.-F. and Lu, F. (2020d), "Predicting Thermophilic Proteins by Machine Learning", *Current Bioinform.*, **15**(5), 493-502. https://doi.org/10.2174/1574893615666200207094357

Wang, X.-p., Li, Z.-c., Sun, T.-c., Kou, J. and Li, X.-h. (2020e), "Factor analysis on the purity of magnesium titanate directly prepared from seashore titanomagnetite concentrate through direct reduction", *Int. J. Minerals Metall. Mater.*, **27**(11), 1462-1470. https://doi.org/10.1007/s12613-020-1990-7

Wang, X., Liu, Y. and Choo, K. (2020f), "Fault tolerant, ulti-subset aggregation scheme for smart grid", *IEEE Transact. Indust. Inform.*

Wu, C., Wang, X., Chen, M. and Kim, M.J. (2019a), "Differential received signal strength based RFID positioning for construction equipment tracking", *Adv. Eng. Inform.*, **42**, 100960. https://doi.org/10.1016/j.aei.2019.100960

Wu, T., Cao, J., Xiong, L. and Zhang, H. (2019b), "New stabilization results for semi-Markov chaotic systems with fuzzy sampled-data control", *Complexity*, 2019. https://doi.org/10.1155/2019/7875305

Wu, C., Wu, P., Wang, J., Jiang, R., Chen, M. and Wang, X. (2020a), "Critical review of data-driven decision-making in bridge operation and maintenance", *Struct. Infrastruct. Eng.*, 1-24. https://doi.org/10.1080/15732479.2020.1833946

Wu, T., Xiong, L., Cheng, J. and Xie, X. (2020b), "New results on stabilization analysis for fuzzy semi-Markov jump chaotic systems with state quantized sampled-data controller", *Inform. Sci.*, **521**, 231-250. https://doi.org/10.1016/j.ins.2020.02.051

Wu, C., Wu, P., Wang, J., Jiang, R., Chen, M. and Wang, X. (2021), "Ontological knowledge base for concrete bridge rehabilitation project management", *Automat. Constr.*, **121**, 103428. https://doi.org/10.1016/j.autcon.2020.103428

Xie, Q., Sinaei, H., Shariati, M., Khorami, M., Mohamad, E.T. and Bui, D.T. (2019), "An experimental study on the effect of CFRP on behavior of reinforce concrete beam column connections", Steel and Composite Structures, 30(5), 433-441. https://doi.org/10.12989/scs.2019.30.5.433

Xu, M., Li, C., Chen, Z., Wang, Z. and Guan, Z. (2018a), "Assessing visual quality of omnidirectional videos", *IEEE Transact. Circuits Syst. Video Technol.*, **29**(12), 3516-3530. https://doi.org/10.1109/TCSVT.2018.2886277

Xu, M., Li, T., Wang, Z., Deng, X., Yang, R. and Guan, Z. (2018b), "Reducing complexity of HEVC: A deep learning approach", *IEEE Transact. Image Process.*, **27**(10), 5044-5059. https://doi.org/10.1109/TIP.2018.2847035

Xu, M., Li, C., Zhang, S. and Le Callet, P. (2020), "State-of-the-art in 360 video/image processing: Perception, assessment and compression", *IEEE J. Select. Topics Signal Process.*, **14**(1), 5-26. https://doi.org/10.1109/JSTSP.2020.2966864

Xue, Q., Zhu, Y. and Wang, J. (2019), "Joint distribution estimation and Naïve Bayes classification under local differential privacy", *IEEE Transact. Emerg. Topics Comput.* https://doi.org/10.1109/TETC.2019.2959581

Yang, M. and Sowmya, A. (2015), "An underwater color image quality evaluation metric", *IEEE Transact. Image Process.*, **24**(12), 6062-6071. https://doi.org/10.1109/TIP.2015.2491020

Yang, R., Xu, M., Liu, T., Wang, Z. and Guan, Z. (2018), "Enhancing quality for HEVC compressed videos", *IEEE Transact. Circuits Syst. Video Technol.*, **29**(7), 2039-2054. https://doi.org/10.1109/TCSVT.2018.2867568

Yang, S., Deng, B., Wang, J., Li, H., Lu, M., Che, Y., Wei, X. and Loparo, K.A. (2019), "Scalable digital neuromorphic architecture for large-scale biophysically meaningful neural network with multi-compartment neurons", *IEEE Transact. Neural Networks Learn. Syst.*, **31**(1), 148-162. https://doi.org/10.1109/TNNLS.2019.2899936

Yang, J., Li, S., Wang, Z., Dong, H., Wang, J. and Tang, S. (2020), "Using Deep Learning to Detect Defects in Manufacturing: A Comprehensive Survey and Current Challenges", *Materials*, **13**(24), 5755. https://doi.org/10.3390/ma13245755

Yu, H., Dai, W., Qian, G., Gong, X., Zhou, D., Li, X. and Zhou, X. (2020a), "The NOx Degradation Performance of Nano-TiO_2 Coating for Asphalt Pavement", *Nanomaterials*, **10**(5), 897. https://doi.org/10.3390/nano10050897

Yu, H., Zhu, X., Qian, G., Gong, X. and Nie, X. (2020b), "Evaluation of phosphorus slag (PS) content and particle size on the performance modification effect of asphalt", *Constr. Build. Mater.*, **256**, 119334. https://doi.org/10.1016/j.conbuildmat.2020.119334

Yue, H., Wang, H., Chen, H., Cai, K. and Jin, Y. (2020), "Automatic detection of feather defects using Lie group and fuzzy Fisher criterion for shuttlecock production", *Mech. Syst. Signal Process.*, **141**, 106690. https://doi.org/10.1016/j.ymssp.2020.106690

Zhang, C. (2014), "Control force characteristics of different control strategies for the wind-excited 76-story benchmark building structure", *Adv. Struct. Eng.*, **17**(4), 543-559. https://doi.org/10.1260/1369-4332.17.4.543

Zhang, W. (2020), "Parameter adjustment strategy and experimental development of hydraulic system for wave energy power generation", *Symmetry*, **12**(5), 711. https://doi.org/10.3390/sym12050711

Zhang, J. and Liu, B. (2019), "A review on the recent developments of sequence-based protein feature extraction methods", *Current Bioinform.*, **14**(3), 190-199. https://doi.org/10.2174/1574893614666181212102749

Zhang, C. and Mousavi, A.A. (2020), "Blast loads induced responses of RC structural members: State-of-the-art review", *Compos. Part B: Eng.*, **195**, 108066. https://doi.org/10.1016/j.compositesb.2020.108066

Zhang, C. and Wang, H. (2019a), "Robustness of the active rotary inertia driver system for structural swing vibration control subjected to multi-type hazard excitations", *Appl. Sci.*, **9**(20), 4391. https://doi.org/10.3390/app9204391

Zhang, C. and Wang, H. (2019b), "Swing vibration control of suspended structure using active rotary inertia driver system: Parametric analysis and experimental verification", *Appl. Sci.*, **9**(15), 3144. https://doi.org/10.3390/app9153144

Zhang, C. and Wang, H. (2020c), "Swing vibration control of suspended structures using the Active Rotary Inertia Driver system: Theoretical modeling and experimental verification", *Struct. Control Health Monitor.*, **27**(6), e2543. https://doi.org/10.1002/stc.2543

Zhang, X., Wang, Y., Chen, X., Su, C.-Y., Li, Z., Wang, C. and Peng, Y. (2018), "Decentralized adaptive neural approximated inverse control for a class of large-scale nonlinear hysteretic systems with time delays", *IEEE Transact. Syst. Man Cybernet.: Syst.*, **49**(12), 2424-2437. https://doi.org/10.1109/TSMC.2018.2827101

Zhang, C., Alam, Z., Sun, L., Su, Z. and Samali, B. (2019a), "Fibre Bragg grating sensor-based damage response monitoring of an asymmetric reinforced concrete shear wall structure subjected to progressive seismic loads", *Struct. Control Health Monitor.*, **26**(3), e2307. https://doi.org/10.1002/stc.2307

Zhang, C., Gholipour, G. and Mousavi, A.A. (2019b), "Nonlinear dynamic behavior of simply-supported RC beams subjected to combined impact-blast loading", *Eng. Struct.*, **181**, 124-142. https://doi.org/10.1016/j.engstruct.2018.12.014

Zhang, H., Qiu, Z., Cao, J., Abdel-Aty, M. and Xiong, L. (2019c), "Event-triggered synchronization for neutral-type semi-Markovian neural networks with partial mode-dependent time-varying delays", *IEEE Transact. Neural Networks Learn. Syst.*, **31**(11), 4437-4450. https://doi.org/10.1109/TNNLS.2019.2955287

Zhang, B., Niu, Z., Wang, J., Ji, D., Zhou, T., Liu, Y., Feng, Y., Hu, Y., Zhang, J. and Fan, Y. (2020a), "Four-hundred gigahertz broadband multi-branch waveguide coupler", *IET Microwaves, Antennas & Propagation*, **14**(11), 1175-1179. https://doi.org/10.1049/iet-map.2020.0090

Zhang, C., Abedini, M. and Mehrmashhadi, J. (2020b), "Development of pressure-impulse models and residual capacity assessment of RC columns using high fidelity Arbitrary Lagrangian-Eulerian simulation", *Eng. Struct.*, **224**, 111219. https://doi.org/10.1016/j.engstruct.2020.111219

Zhang, C., Chen, Z., Wang, J., Liu, Z. and Chen, C.P. (2020c), "Fuzzy adaptive two-bit-triggered control for a class of uncertain nonlinear systems with actuator failures and dead-zone constraint", *IEEE Transac. Cybernetics*, **51**(1), 210-221. https://doi.org/10.1109/TCYB.2020.2970736

Zhang, C., Gholipour, G. and Mousavi, A.A. (2020d), "State-of-the-Art Review on Responses of RC Structures Subjected to Lateral Impact Loads", *Arch. Computat. Methods Eng.*, 1-31. https://doi.org/10.1007/s11831-020-09467-5

Zhang, J., Chen, Q., Sun, J., Tian, L. and Zuo, C. (2020e), "On a universal solution to the transport-of-intensity equation", *Optics Letters*, **45**(13), 3649-3652. https://doi.org/10.1364/OL.391823

Zhang, J., Sun, J., Chen, Q. and Zuo, C. (2020f), "Resolution analysis in a lens-free on-chip digital holographic microscope", *IEEE Transact. Computat. Imag.*, **6**, 697-710. https://doi.org/10.1109/TCI.2020.2964247

Zhang, R., Jiang, T., Li, F., Li, G., Chen, H. and Li, X. (2020g), "Coordinated bidding strategy of wind farms and power-to-gas facilities using a cooperative game approach", *IEEE Transact. Sustain. Energy*, **11**(4), 2545-2555. https://doi.org/10.1109/TSTE.2020.2965521

Zhang, S., Pak, R.Y. and Zhang, J. (2020h), "Vertical time-harmonic coupling vibration of an impermeable, rigid, circular plate resting on a finite, poroelastic soil layer", *Acta Geotech.*, **16**, 911-935. https://doi.org/10.1007/s11440-020-01067-8

Zhang, T., He, X., Deng, Y., Tsang, D.C., Yuan, H., Shen, J. and Zhang, S. (2020i), "Swine manure valorization for phosphorus and nitrogen recovery by catalytic–thermal hydrolysis and struvite crystallization", *Sci. Total Environ.*, **729**, 138999. https://doi.org/10.1016/j.scitotenv.2020.138999

Zhang, W., Tang, Z., Yang, Y. and Wei, J. (2021), "Assessment of FRP–Concrete Interfacial Debonding with Coupled Mixed-Mode Cohesive Zone Model", *J. Compos. Constr.*, **25**(2), 04021002. https://doi.org/10.1061/(ASCE)CC.1943-5614.0001114

Zhao, H., Li, Y., Song, Q., Liu, S., Ma, Q., Ma, L. and Shu, X. (2019), "Catalytic reforming of volatiles from co-pyrolysis of lignite blended with corn straw over three different structures of

iron ores", *J. Anal. Appl. Pyrol.*, **144**, 104714. https://doi.org/10.1016/j.jaap.2019.104714

Zhao, J., Liu, J., Jiang, J. and Gao, F. (2020), "Efficient Deployment with Geometric Analysis for mmWave UAV Communications", *IEEE Wireless Commun. Lett.*, **9**(7), 1115-1119. https://doi.org/10.1109/LWC.2020.2982637

Zhu, L., Zhang, C., Guan, X., Uy, B., Sun, L. and Wang, B. (2018), "The multi-axial strength performance of composited structural B-C-W members subjected to shear forces", *Steel Compos. Struct., Int. J.*, **27**(1), 75-87. https://doi.org/10.12989/scs.2018.27.1.075

Zhu, J., Wang, X., Chen, M., Wu, P. and Kim, M.J. (2019a), "Integration of BIM and GIS: IFC geometry transformation to shapefile using enhanced open-source approach", *Automat. Constr.*, **106**, 102859. https://doi.org/10.1016/j.autcon.2019.102859

Zhu, J., Wang, X., Wang, P., Wu, Z. and Kim, M.J. (2019b), "Integration of BIM and GIS: Geometry from IFC to shapefile using open-source technology", *Automat. Constr.*, **102**, 105-119. https://doi.org/10.1016/j.autcon.2019.02.014

Zhu, L., Kong, L. and Zhang, C. (2020), "Numerical study on hysteretic behaviour of horizontal-connection and energy-dissipation structures developed for prefabricated shear walls", *Appl. Sci.*, **10**(4), 1240. https://doi.org/10.3390/app10041240

Ziaei-Nia, A., Shariati, M. and Salehabadi, E. (2018), "Dynamic mix design optimization of high-performance concrete", *Steel Compos. Struct., Int. J.*, **29**(1), 67-75. https://doi.org/10.12989/scs.2018.29.1.067

Zuo, C., Chen, Q., Tian, L., Waller, L. and Asundi, A. (2015), "Transport of intensity phase retrieval and computational imaging for partially coherent fields: The phase space perspective", *Optics Lasers Eng.*, **71**, 20-32. https://doi.org/10.1016/j.optlaseng.2015.03.006

Zuo, C., Sun, J., Li, J., Zhang, J., Asundi, A. and Chen, Q. (2017), "High-resolution transport-of-intensity quantitative phase microscopy with annular illumination", *Scientif. Reports*, **7**(1), 7654. https://doi.org/10.1038/s41598-017-06837-1

Zuo, C., Li, J., Sun, J., Fan, Y., Zhang, J., Lu, L., Zhang, R., Wang, B., Huang, L. and Chen, Q. (2020a), "Transport of intensity equation: a tutorial", *Optics Lasers Eng.*, 106187. https://doi.org/10.1016/j.optlaseng.2020.106187

Zuo, C., Sun, J., Li, J., Asundi, A. and Chen, Q. (2020b), "Wide-field high-resolution 3d microscopy with fourier ptychographic diffraction tomography", *Optics Lasers Eng.*, **128**, 106003. https://doi.org/10.1016/j.optlaseng.2020.106003